

See discussions, stats, and author profiles for this publication at: <https://www.researchgate.net/publication/287546509>

The Population Biology of Abalone (*Haliotis* species) in Tasmania. I. Blacklip Abalone (*H. rubra*) from the North Coast and Islands of Bass Strait

Article · January 1994

CITATIONS

136

READS

2,694

5 authors, including:



Warwick J. Nash

26 PUBLICATIONS 1,374 CITATIONS

SEE PROFILE

TECHNICAL REPORT NO. 48

The Population Biology of Abalone
(*Haliotis* species) in Tasmania.
I. Blacklip Abalone (*H. rubra*) from the
North Coast and the Islands
of Bass Strait

Warwick J. Nash, Tracy L. Sellers, Simon R. Talbot,
Andrew J. Cawthorn and Wes B. Ford

1994



SEA FISHERIES DIVISION
MARINE RESEARCH LABORATORIES - TAROONA
DEPARTMENT OF PRIMARY INDUSTRY AND FISHERIES, TASMANIA

TECHNICAL REPORT NO. 48

The Population Biology of Abalone (*Haliotis* species) in Tasmania. I. Blacklip Abalone (*H. rubra*) from the North Coast and the Islands of Bass Strait

Warwick J. Nash, Tracy L. Sellers, Simon R. Talbot,
Andrew J. Cawthorn and Wes B. Ford

1994

SEA FISHERIES DIVISION
MARINE RESEARCH LABORATORIES - TAROONA
DEPARTMENT OF PRIMARY INDUSTRY AND FISHERIES, TASMANIA

National Library of Australia Cataloguing-in-Publication Entry

The Population Biology of Abalone (*Haliotis* species) in Tasmania. I. Blacklip Abalone (*H. rubra*) from the North Coast and the Islands of Bass Strait.

Bibliography.
ISBN 0 7246 4144 0.

1. Abalones - Tasmania. 2. Abalones - Size - Tasmania.
3. Abalones - Bass Strait. 4. Abalones - Size - Bass
Strait. 5. Abalone culture - Tasmania. 6. Abalone
culture - Bass Strait. 7. Invertebrate populations -
Tasmania. 8. Invertebrate populations - Bass Strait. I.
Nash, Warwick J. II. Tasmania. Marine Laboratories.
(Series: Technical report (Tasmania. Marine
Laboratories); 48).

594.3

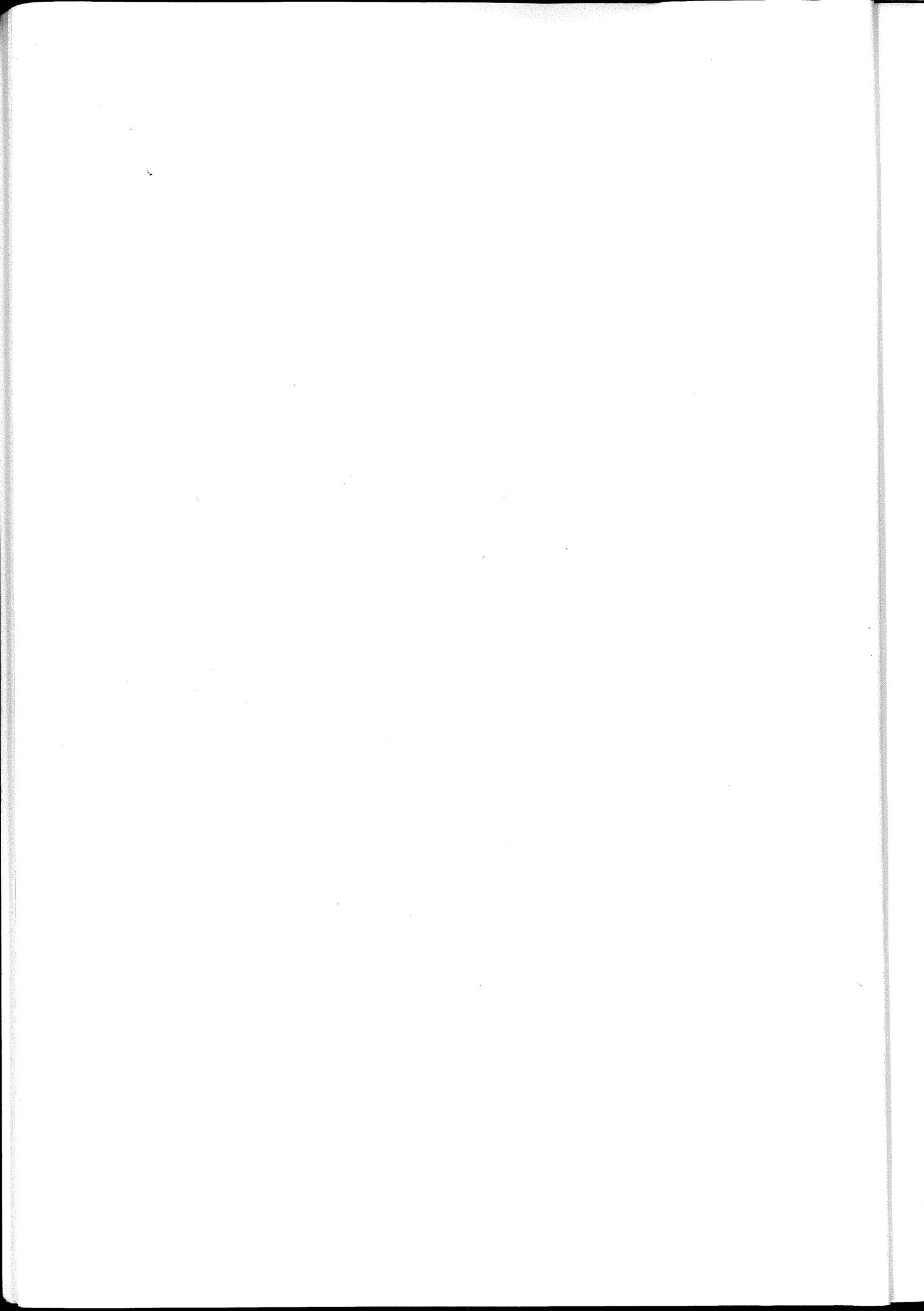
Published by the Sea Fisheries Division, Marine Research Laboratories - Taroona,
Department of Primary Industry and Fisheries, Tasmania 1994

Series Editor - Dr Jeremy Lyle

The opinions expressed in this report are those of the authors and are not necessarily those of the Sea Fisheries Division or the Department of Primary Industry and Fisheries, Tasmania.

CONTENTS

	Page
Abstract	1
1 Introduction	1
2 Methods	4
2.1 Field procedures	4
2.2 Laboratory and analytical procedures	8
2.2.1 Morphometrics	8
2.2.2 Ageing and growth	9
2.2.3 Sexual maturation	10
2.2.4 Fecundity estimation	11
2.2.5 Mortality estimation	13
2.2.6 Yield per recruit	14
2.2.7 Egg per recruit	15
3 Results	16
3.1 Morphometrics	16
3.2 Age and growth	19
3.3 Sexual maturation and fecundity	31
3.3.1 Onset of sexual maturity	31
3.3.2 Fecundity	31
3.4 Cryptic and emergent abalone	38
3.5 Mortality	38
3.6 Yield per recruit	46
3.7 Egg per recruit	51
4 Discussion	51
4.1 Morphometrics	51
4.2 Growth and ageing	54
4.3 Sexual maturation and fecundity	55
4.3.1 Onset of sexual maturity	55
4.3.2 Fecundity	56
4.4 Mortality	58
4.5 Yield per recruit and egg per recruit	61
5 Acknowledgements	61
6 References	62
Appendix I	65



ABSTRACT

Surveys of stunted blacklip abalone (*Haliotis rubra*) were carried out in five areas in Bass Strait in order to obtain biological information that could be used to determine, among other things, an appropriate legal minimum size for these stocks. Growth checks and layers in the shell were used to age the abalone assuming the one-layer-per-year relationship established for *H. rubra* in southern Tasmania. The degree of stunting, assessed using the maximum shell diameter and the age-length relationship, was greatest in the Kent Islands and Waterhouse Island, and less pronounced at the Hogan Islands, Babel Island and Cape Barren Island. This was reflected in the size at onset of sexual maturity: size at 50 percent maturity ranged from 65.3 mm at Waterhouse Island to 82.6 mm at the Hogan Islands.

Analysis of residuals showed that fecundity is clearly size-related, with a poor relationship between age and fecundity.

Estimates of instantaneous total mortality (Z) of fully recruited age classes, derived by catch curve analysis, ranged from 0.185 to 0.265. Yield-per-recruit (YPR) analysis showed that the size at maximum yield per recruit was less than 100 mm at all sites—considerably less than the 118 mm and 110 mm size limits that have applied to this stunted fishery in one-month fishing exercises in 1989, 1991 and 1993. Egg-per-recruit (EPR) analysis was carried out to determine the proportion of the virgin egg production that would be conserved at various combinations of size at first capture and fishing mortality. YPR and EPR analyses were repeated using several assumed levels of instantaneous natural mortality (M) ($M=Z$, $M=0.75*Z$, and $M=0.5*Z$), and number of shell layers per year (either 1 or 2). Several M values were applied because an unknown amount of illegal fishing of the Bass Strait abalone stocks by Victorian divers occurs; they were essentially unfished by Tasmanian divers prior to the 1989 stunted fishing exercise because only a very small proportion grow larger than the 132 mm size Tasmanian size limit. Both YPR and EPR results were found to be sensitive to variation in M alone: size at maximum YPR increased, while EPR decreased, as M decreased. YPR was shown to be moderately sensitive to the rate of shell layer deposition (whether one or two per year), but the effect on EPR was only slight at size at first capture $\geq c. 100$ mm. The relative insensitivity of EPR to the number of growth rings deposited in the shell per year is attributed to the fact that the value of Z for two rings per year is twice that for one ring per year; countervailing this, growth rates are doubled—the von Bertalanffy growth parameters change by a factor of two: K doubles and t_0 is halved. This insensitivity of EPR to the rate of shell layer deposition is important because it enables a reasonably accurate assessment of the impact of fishing on population egg production to be made even when this relationship is unknown. A requisite assumption—that the relationship between shell layers and age be linear—is supported by circumstantial evidence provided by the observed pattern of mean size of mature and immature abalone within a putative age class.

1 INTRODUCTION

Abalone are marine snails that generally have aggregated distributions. Blacklip abalone (*Haliotis rubra* Leach) inhabit complex rocky substrate (with ledges, crevices and overhangs) more often than featureless, flat rocky pavement. Within the preferred habitat, some particular places appear to be especially preferred by abalone, as indicated by the high recovery rates in these places following fishing. The features of these so-called ‘hot spots’ that make them attractive to abalone are unknown, but are probably associated with availability of food (drift algae) and reproduction. The seasonal nature of some of these aggregations, and their coincidence with the time of peak reproductive condition, suggest that abalone aggregate at some particular places to spawn.

The existence of these aggregations, and the targeting of these aggregations by experienced abalone divers, has important implications for assessing the condition of an abalone stock. Abalone continue to move to the 'hot spots' as they are depleted by fishing; as a result, there is little change in catch rates until the number of abalone remaining to move into these 'hot spots' has very largely diminished. Consequently, divers' catch rates are insensitive to changes in abalone abundance. The mechanics of this have been described by Hilborn and Walters (1987), Prince (1987) and Sloan and Breen (1988). In this sense abalone are similar to schooling fish, for which changes in catch rate are also insensitive to changes in stock abundance, unless searching time, as well as fishing time, is taken into account. As a result, stable catch rates are not unequivocal evidence that overfishing is not occurring.

Until at least mid-1988, commercial abalone divers had been stating that the number of abalone seen on the bottom while diving continued to decrease, at least in some areas. Until the realisation that catch rates are insensitive to changes in stock abundance, little credence was given to these opinions. No other measurements of stock abundance or changes in stock abundance through time had been hitherto conducted. On the basis of available information and analyses it was impossible to determine whether the abalone stocks in Tasmania were being overfished.

In order to obtain qualitative information on the state of the abalone stocks, one of us (WN) interviewed, in early 1988, several divers who had been fishing for 15 years or more. Long-term divers were targetted because their time in the fishery enabled them to have a greater perspective on changes in abalone abundance, as perceived while diving for abalone.

Most of the divers interviewed stated that, not only had stocks decreased greatly since they first entered the fishery, but that this decline was continuing; abalone were considered to be less abundant than they were even four or five years previously. Clearly, the abundance of abalone will decline as the accumulation of old animals is removed from the virgin stock; this is a normal (and unavoidable) consequence of fishing. But continuing decline in number of adults suggests that the stocks are being overfished. If these diver observations are combined with the fact that total annual catches in the second decade of the fishery have been substantially higher than those in the first decade (Fig. 1), there is good cause to believe that stocks may be declining.

An unpublished discussion paper containing these arguments was written by the senior author. It provoked serious discussion among abalone divers, processors and Department of Sea Fisheries' personnel. Following lengthy discussions and negotiations between industry and government, and a vote by members of the Tasmanian Abalone Divers Association (TADA) that

quota be reduced by 30 percent, the Minister for Sea Fisheries announced, in November 1988, that the total annual catch for 1989 was to be reduced to 70 percent of the 1988 catch (to 2,100 tonnes live weight).

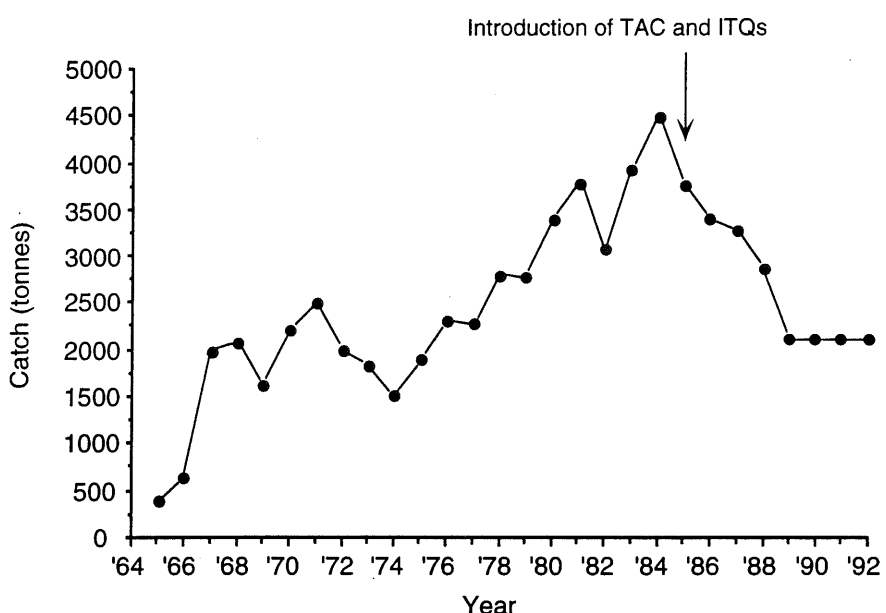


Figure 1. Tasmanian abalone catch statistics for 1965 to 1992.

Because of the adverse financial effects that such a reduction in diver and processor income may have caused, particularly on those divers who had recently bought a licence, the TADA argued that blacklip abalone (*Haliotis rubra*) stocks in the north of the State be made accessible to divers at a reduced size limit, and that each diver be allowed to catch an extra four units of abalone (equivalent to 2.4 tonnes live weight) upon issue of an Exploratory Licence. This request had a biologically sound basis, because *H. rubra* decrease in maximum size (and hence presumably growth rate) from south to north (Nash 1992). In some areas, *H. rubra* does not even reach the present lower legal size limit of 132 mm maximum shell diameter. These northern stocks therefore were essentially unexploited.

Access to these stocks was denied at that time, however, because of the lack of biological information concerning an appropriate size limit. The TADA therefore offered its services to carry out the necessary survey of the northern abalone populations so that the exploratory opening could proceed at a biologically determined reduced size limit. This document reports the results of that survey. One-month fishing exercises at a reduced size limit in Bass Strait waters have subsequently taken place, in 1989, 1991 and 1993.

This survey was also the first of several to document the population profiles of *Haliotis rubra* in Tasmanian waters. Information gained or adduced from these surveys includes length-at-age,

age and length at maturity, age- and length-fecundity relationships, estimates of natural and total mortality, and finally yield-per-recruit and egg-per-recruit analyses to determine size limits at different levels of fishing pressure that are appropriate to maintain (or achieve) optimal yields and egg production.

2 METHODS

2.1 Field procedures

The survey of the Bass Strait islands was undertaken over three days, from May 31 to June 2, 1988. The 29-metre commercial abalone vessel *Kobus* was used as mother ship. Abalone populations were surveyed in five areas: the Hogan and Kent groups of islands, Babel Island and Cape Barren Island, as well as from Waterhouse Island and the adjacent Tasmanian coastline (Fig. 2). Thirty-eight sites were surveyed. Exact locations of these sites are shown in Figs. 3 to 7. Because the survey was of blacklip abalone, only blacklip habitat was visited. A small number of greenlip abalone (*H. laevigata*) found in these areas were also collected.

The survey was carried out by three teams, each consisting of a commercial diver, a Department of Sea Fisheries (DSF) diver and a deckhand, each operating from a 4.3 m dinghy. Each team surveyed one or more sites per area, depending on geographical and time constraints. The sampling procedure was as follows: At each site, the commercial diver collected all abalone, regardless of size, that could be found in exposed positions, while the DSF diver searched for cryptic abalone under boulders and deep in cracks and crevices. Cryptic abalone were defined as those which could not be seen without turning boulders or otherwise exposing them; emergent abalone were the remainder. Previous studies of blacklip abalone from the north coast of Tasmania (unpublished data) had shown that a sample size of at least 200 animals, encompassing the entire size range, was necessary to establish the age-length relationship. This is because of the large variation in growth rates between individual abalone, and also because a varying but often large proportion (up to 80 percent) of the blacklip abalone from northern Tasmanian waters is impossible to age by the technique described below, because of extensive damage to the shell by boring sponges.

Since the exposed abalone were generally found more quickly, the commercial diver assisted the DSF diver to collect cryptic abalone once sufficient emergent abalone had been collected. Where possible, cryptic and emergent abalone were kept separate throughout. This was done so that the size, age and state of sexual maturation at which the abalone make the transition from cryptic to emergent behaviour could be determined. Prince *et al.* (1988b) suggested that abalone emerge from the sub-boulder or crevice habitat at the onset of sexual maturity, which is thought

to be age-related rather than size-related. By comparing the age, size and state of sexual maturation of cryptic and emergent abalone, this hypothesis could be evaluated.

All abalone collected were taken back to the mother ship, where they were frozen at -30°C until return to Hobart, where they were stored at -60°C at the Department of Sea Fisheries Taroona laboratories until processed.

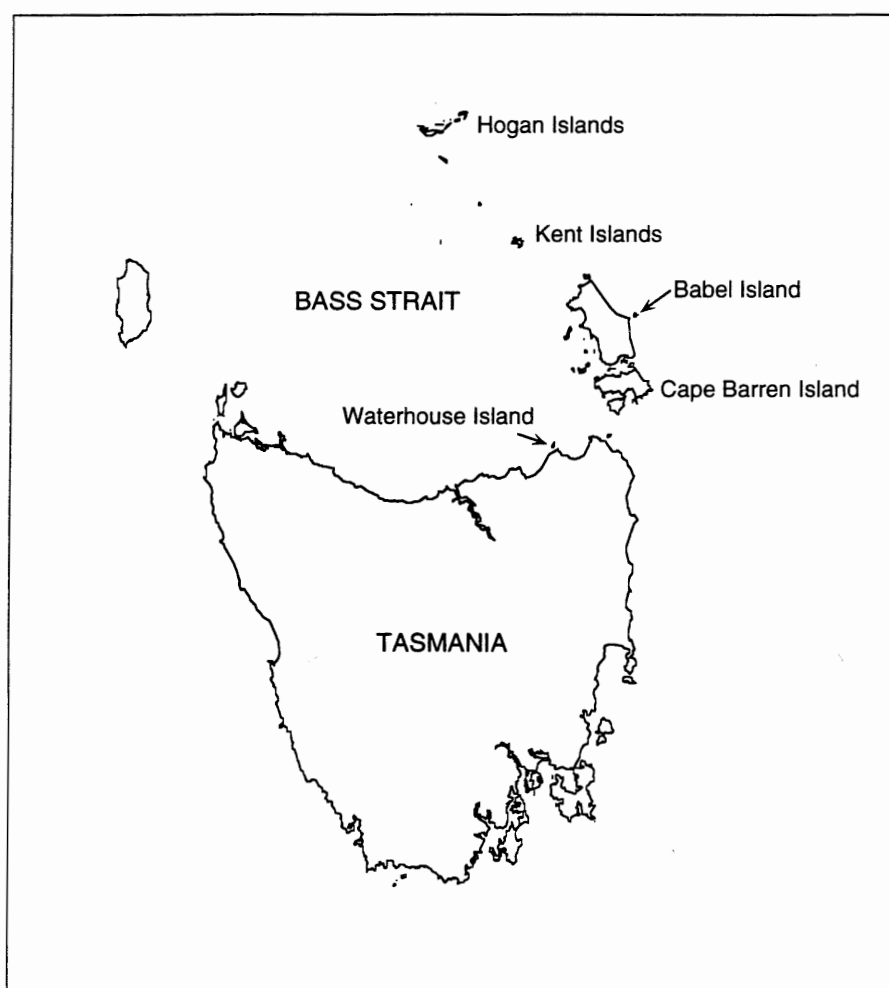


Figure 2. Tasmania and Bass Strait, showing the five survey areas.

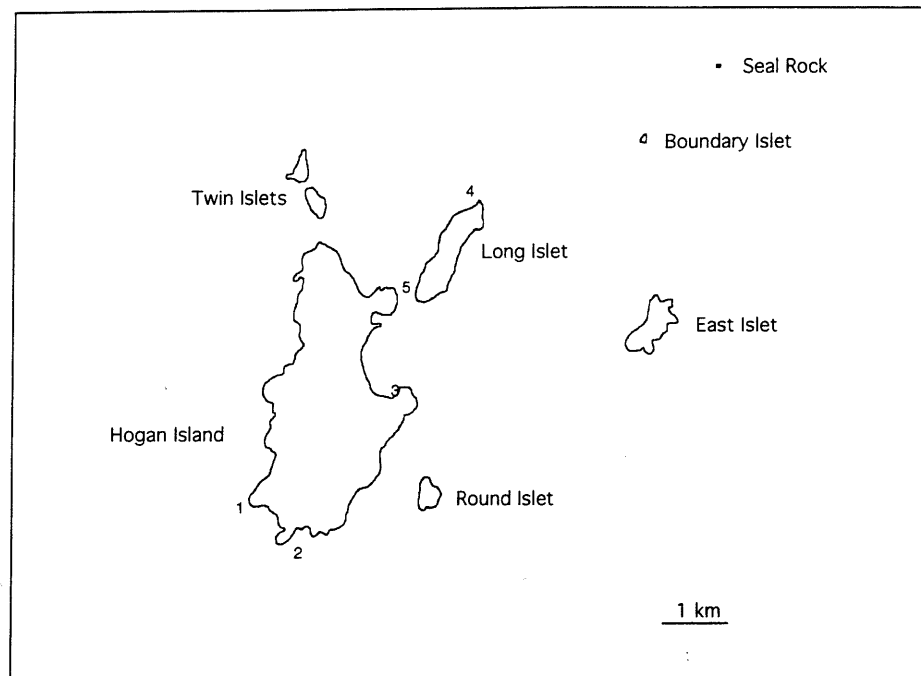


Figure 3. Survey sites at the Hogan Islands

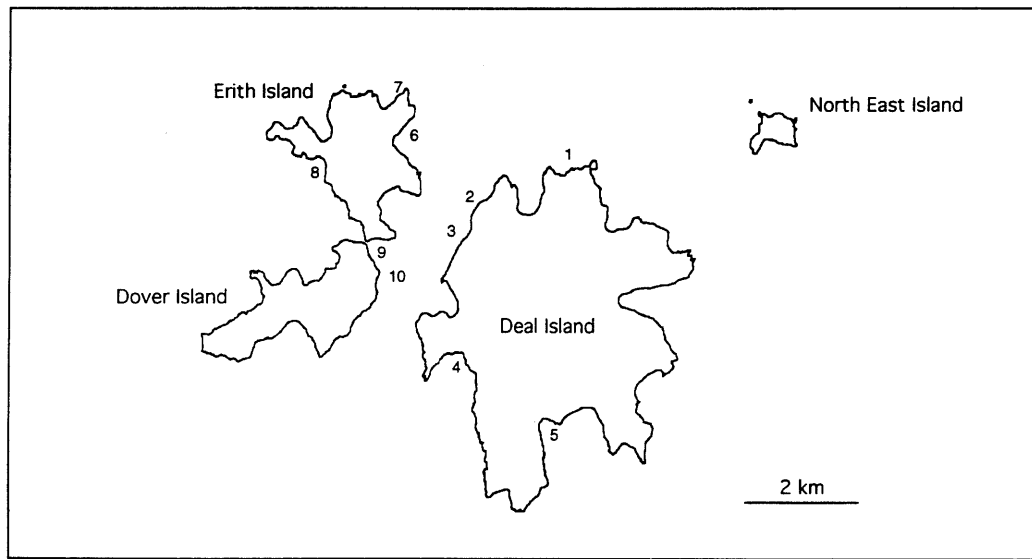


Figure 4. Survey sites at the Kent Islands

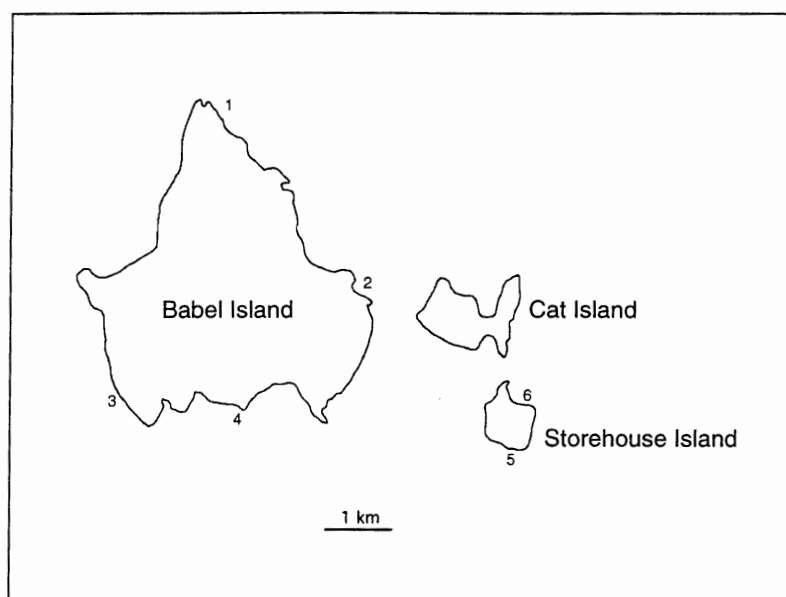


Figure 5. Babel Island survey sites.

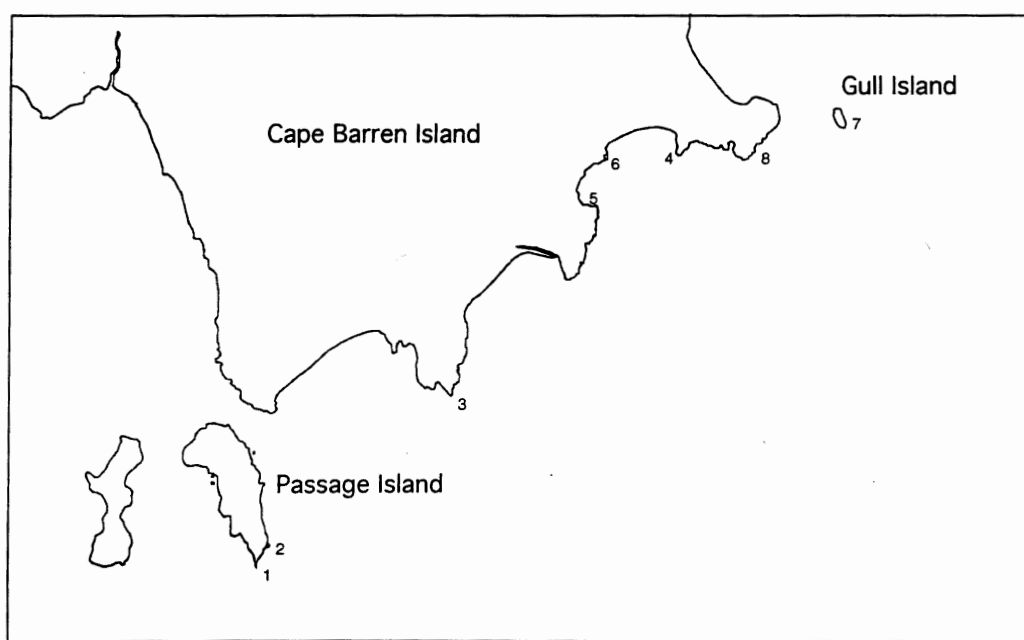


Figure 6. Cape Barren Island survey sites.

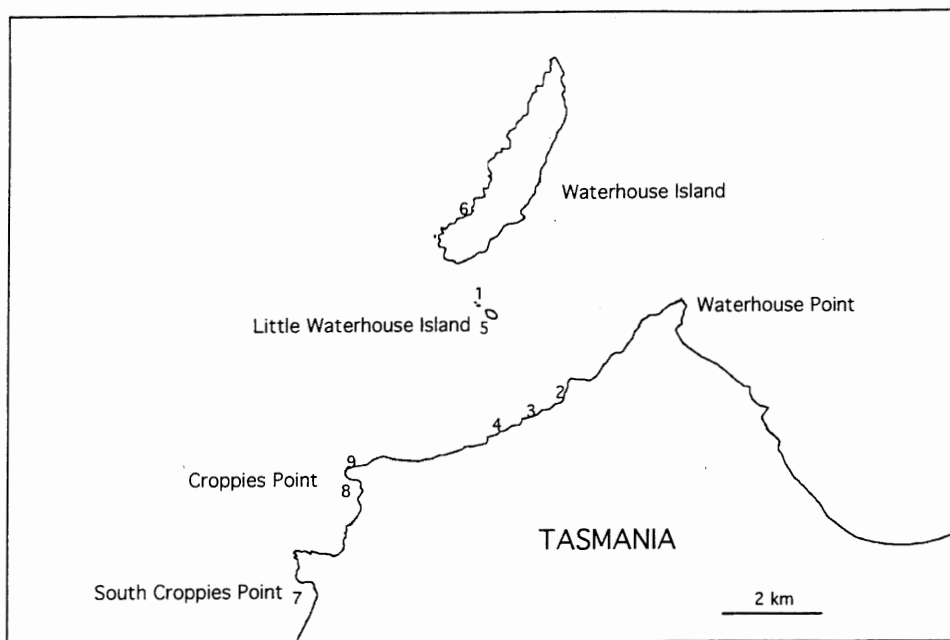


Figure 7. Survey sites at Waterhouse Island and the adjacent Tasmanian shore.

2.2 Laboratory and analytical procedures

Survey data from each dive site sampled were pooled for each of the five areas sampled; within-area variation is not examined here.

2.2.1 Morphometrics

The following measurements were recorded for each abalone: whole weight, shucked meat weight, viscera weight, dry shell weight, maximum shell length, minimum shell length and vertical shell height. Shells were dried to constant weight at 90°C before weighing.

Morphometric relationships were analysed by either simple linear regression—*e.g.*,

$$\text{fecundity} = a + b \cdot \text{whole weight}$$

or fitting non-linear data to the power equation—*e.g.*,

$$\text{whole wt.} = a \cdot \text{length}^b \quad (1)$$

Linearity of the relationship between two variables was tested by log-transformation of the power relationship $y = a \cdot x^b$:

$$\log_e(y) = \log_e(a) + b \cdot \log_e(x).$$

If the relationship being examined is linear, the exponent b does not differ significantly from 1.

2.2.2 Ageing and growth

A technique developed by Muñoz Lopez (1976) for ageing abalone from growth checks in the shell has been shown by Prince *et al.* (1988a) to be valid for *Haliotis rubra* at two sites in south-east Tasmania, one a slow-growing, ‘stunted’ population, the other ‘normal’. Three distinct minor layers are laid down in the first 16 months of life, with subsequent major layers being deposited annually. These layers, visualised as growth rings by grinding flat the apical spire from each shell until a small hole has been formed, are highlighted by acid etching and staining. Age was therefore calculated as the number of major rings present, plus 1.5 years to account for the period during which the minor rings are deposited. Prince (1989) showed that the growth curves obtained by this ageing method, and independently by mark-recapture methods, were virtually identical.

The validity of the application of Prince *et al.*’s findings to *Haliotis rubra* populations beyond south-east Tasmania is unknown; however, the fact that it was found to apply at two sites with different growth rate characteristics suggested that it may be applicable to the stunted *H. rubra* populations of Bass Strait. In case the rate of shell layer deposition is higher, as studies in Victoria suggest (McShane and Smith 1992), most of the analyses described in this report were done with both one and two major growth rings per year, in order to examine their sensitivity to these parameters.

The relationship between age and number of growth rings determines the value of growth parameters and total mortality (when derived by catch curve analysis), which in turn affects the results of other analyses, including yield- and egg-per-recruit. Unless stated otherwise, age (in years) has been calculated as the number of major growth rings plus 1.5, following Prince *et al.* (1988a).

It was found (see Results below) that growth of *Haliotis rubra*, in both length and weight, is sigmoidal when expressed as a function of age. Sigmoidal growth signifies that the rate of growth (expressed in absolute terms, such as mm.yr⁻¹) increases from birth to a maximum at the age corresponding to the inflection point on the growth curve; from this age onwards, the rate of growth declines asymptotically to L_∞ .

Because the von Bertalanffy growth function

$$L_t = L_\infty \cdot [1 - e^{-K(t-t_0)}]$$

describes growth which declines monotonically from birth, it can only be used to describe that portion of a sigmoid growth curve to the right of the inflection point. When the von Bertalanffy growth function is fitted to sigmoid growth curves, the extrapolation of the growth curve to the horizontal (age) axis yields a positive value of t_0 , the theoretical age at which length equals 0 if the animals had grown according to the von Bertalanffy growth function since birth.

The age-length couplets for *Haliotis rubra* from each of the sites were fitted to the Gompertz growth function as well as the von Bertalanffy growth function because the Gompertz function

$$l_t = l_0 \cdot e^{G(1-e^{-gt})},$$

describes sigmoid growth. The parameters of the Gompertz growth function are as follows: l_t is length at time t , measured from a conventional zero at the time the fish would have been of length l_0 ; $G.g$ is the instantaneous rate of growth when $t=0$ and $l=l_0$; g is the instantaneous rate of decrease of the instantaneous rate of growth; and the upper asymptote (L_∞) = $l_0 \cdot e^G$ when t is indefinitely large (Ricker 1975). The inflection point is e^{-1} (=0.368) of the vertical distance from the lower to the upper asymptote.

The age-length data couplets were fitted to the Gompertz and von Bertalanffy growth functions by non-linear least squares using the FISHPARM program of Prager *et al.* (1987).

2.2.3 Sexual maturation

Sexual condition (whether male, female or immature) was determined for each abalone by visual inspection of the intact gonad. Cases of uncertain sexual identity were resolved by microscopic examination of the intact gonad.

Rates of maturation by size and by age were determined by fitting the maturation data to the logistic equation

$$p = \frac{e^{a+b \cdot x}}{1 + e^{a+b \cdot x}} \quad (2)$$

where p is proportion mature, x is length (or age), and a and b are parameters of the logistic function.

2.2.4 Fecundity estimation

Fecundity may be measured in several ways. The ideal measure is the number of eggs spawned per individual female per year. Because this is generally impossible to measure, it is usually measured as the number of ripe eggs in the gonad, the weight of the gonad (either fresh or the ash-free dry weight), or as gonad volume. Gonad volume was initially used in this study. However, since measuring gonad volume is very time-consuming, the cross-sectional area of the gonad taken at the base of the conical appendage (Fig. 8) was used as an index of gonad volume. The validity of this was established by demonstrating that gonad area is closely and linearly related to gonad volume (Fig. 9). Following fixation of the conical appendage in 10 per cent formalin-calcium-acetic acid fixative, the gonad was carefully peeled from the digestive gland, and gonad volume was measured by displacement to the nearest 0.05 ml using the apparatus shown in Fig. 10. Linearity of the relationship between gonad volume and gonad area (Fig. 9) was confirmed: the slope of the regression line of $\log(\text{gonad area})$ on $\log(\text{gonad volume})$ did not differ significantly from 1 ($\alpha=0.05$).

The cut surface of the conical appendix was pressed lightly against a sheet of glass, and the outlines of the gonad and digestive gland traced onto a sheet of transparent plastic overlying the glass (Fig. 8). In a proportion of the abalone, the gonad, although visible, was only a thin veneer of tissue over the digestive gland, so that although sex could be determined, the thickness of the gonad section was too fine relative to the thickness of the pen used to trace it. Because histological examination of gonad tissue has shown that gonads with only a veneer of tissue over the digestive gland are invariably immature (unpublished data), these were excluded from the age- and length-fecundity analyses. Abalone were considered to be sexually differentiated if gonad (either testis or ovary) could be discerned.

The tracings of the cross-sections of the conical appendages were transferred to computer using an optical scanner, and the cross-sectional areas of gonad and digestive gland measured using a graphics computer program.

Although gonad volume does not allow the determination of egg numbers spawned, it does allow the relationship between abalone size and potential fecundity, or abalone age and potential fecundity, to be determined. For the purposes of population and egg-per-recruit analyses, it is the *relative* fecundity between size or age classes, rather than the absolute fecundity, that is important.

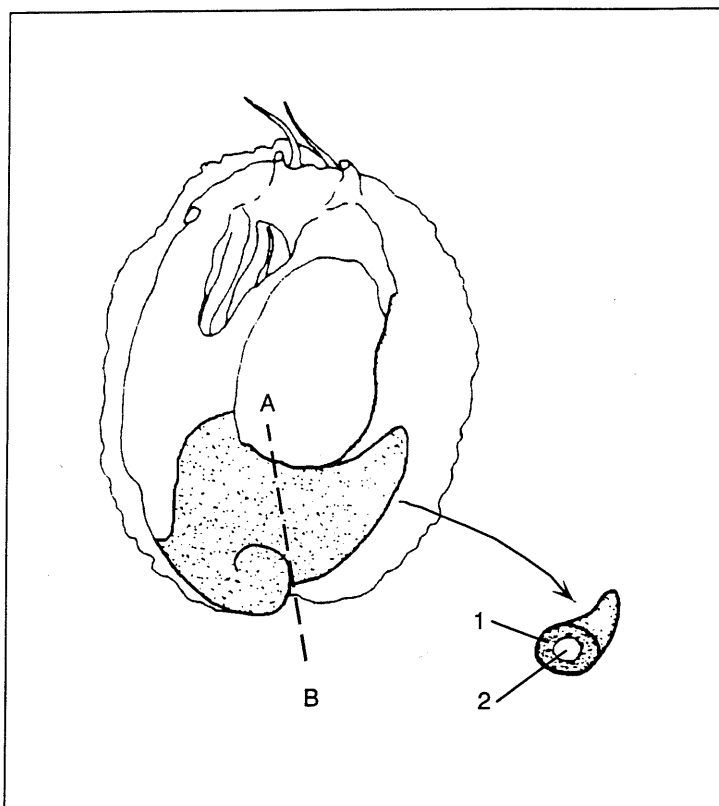


Figure 8. Diagram of the dorsal surface of an abalone with the shell removed, showing the gonad (stippled) and the plane of sectioning of the gonad for analysis (A—B). 1 gonad; 2 digestive gland. Modified after Clavier and Richard (1985).

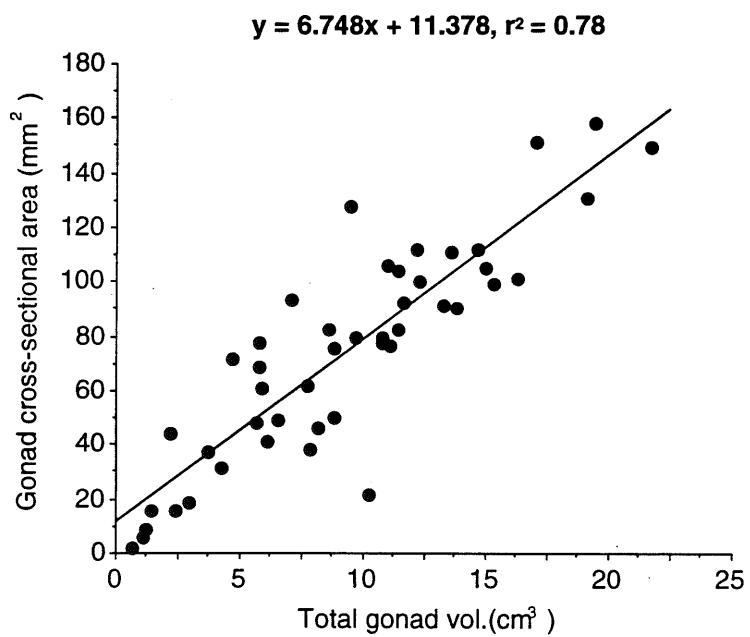


Figure 9. Relationship between gonad volume and gonad cross-sectional area for *Haliotis rubra*, measured at the base of the conical appendage.

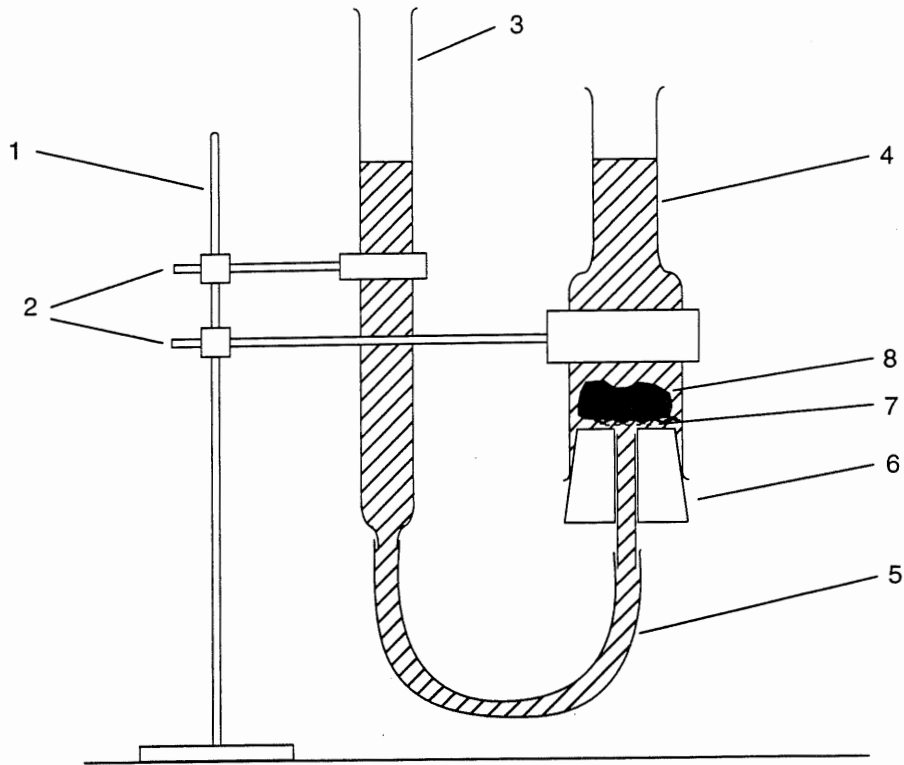


Figure 10. Apparatus used to measure gonad volume by the displacement method.

1 burette stand; 2 burette clamps; 3 graduated 50 ml burette; 4 gonad chamber; 5 flexible rubber tubing; 6 rubber stopper; 7 fine mesh to prevent the loss of gonad tissue down the flexible rubber tubing; 8 gonad tissue.

2.2.5 Mortality estimation

Instantaneous total mortality (Z) was measured by catch curve analysis: the number of animals in each age class [$\log_e(x+1)$ -transformed] was plotted against age, and the slope of the regression line fitted to those age classes that are fully represented in the sample is equal to the instantaneous rate of total mortality (Z) of that population (with the sign of the slope changed). This is strictly correct only in a population with stable age structure (constant rates of recruitment through time) and constant age-specific mortality rates. The extent to which these conditions may be violated, and the effects such violations have on total mortality determination, are discussed in Section 4.4 below. Two values of Z were obtained, using the alternative assumptions of one and two growth rings per year.

Robson and Chapman (1961) proposed that the regression line be fitted to those points to the right of the highest point (P_{max}) on the catch curve; P_{max} should be excluded because of incomplete recruitment effects. This procedure was adopted unless P_{max} lay above the leftward projection of the regression line that did not include P_{max} because this indicates that recruitment is complete (Pauly 1991).

i in this case P_{max} was included in the regression as the first data point.

In an unfished population (when $F = 0$), the total mortality equals the natural mortality. Although abalone are fished throughout all Tasmanian coastal waters, there are some areas where fishing pressure is very low, and from which estimates of natural mortality could therefore be obtained. One of these is the north coast of Tasmania, particularly between Rocky Cape and Waterhouse Island, and the islands of Bass Strait, where the growth rates and maximum sizes are much lower than in other parts of Tasmania. In this area, blacklip abalone hardly (not at all in some areas) reach the minimum legal length of 132 mm. Hence, the fishing mortality of these abalone is very low, and for the purposes of this study may be considered to be zero. Because yield- and egg-per-recruit analyses, among others, require an estimate of M , obtaining an estimate of this parameter is very important.

The extent to which the assumption of zero fishing mortality of *Haliotis rubra* populations in Bass Strait is violated by the taking of undersized abalone by either Tasmanian or inter-State divers is not known. This is evaluated further below by determining the sensitivity of both yield- and egg-per-recruit analyses to variation in natural mortality (M). Three levels of M were used: $M=Z$, $M=0.75*Z$ and $M=0.5*Z$. Although the extent of fishing (either legal or illegal) in these Bass Strait islands is unknown, it is likely that the upper value of F used in these analyses ($F=M=0.5*Z$) is a realistic upper limit.

2.2.6 Yield per recruit

Yield-per-recruit (YPR) analyses were conducted to examine the yield per recruit from the fishery, relative to the maximum yield (B_{max}) that could be obtained from the stock, at different combinations of fishing mortality (F) and minimum size limit (l_C).

Data required for the YPR analyses are the von Bertalanffy growth parameters (L_∞ , K and t_0), maximum age (t_λ), instantaneous natural mortality coefficient (M), the length-weight relationship (Equation 1) and the parameters of the logistic maturation curve (Equation 2), which was used as the selection coefficient (see below).

Yield per recruit was expressed as a percentage of the maximum biomass attained by a cohort (B_{max}), and calculated using the equation:

$$YPR = \frac{1}{B_{max}} \cdot 100 \cdot \sum_{t=t_R}^{t_\lambda} \frac{F \cdot q_t}{F \cdot q_t + M} \cdot N_t \cdot W_t \cdot (1 - e^{-(F \cdot q_t + M)})$$

where t_R is the age at first capture (recruitment to the fishery), t_λ is longevity (in years), measured as the maximum age attained by abalone in the population, F and M are the instantaneous rates of fishing and natural mortality respectively, W_t is the whole weight of an abalone of age t , and N_t , the number of abalone surviving to time t , is calculated as

$$N_t = N_{t-1} \cdot e^{-(F \cdot q_{t-1} + M)}$$

The size-specific selection coefficient (q) was calculated as the proportion of each length class that is sexually mature, using Equation (2) above. (The age-specific maturation ogive could have been applied with equal validity.) The maturation ogive was applied as the selection coefficient because, as described in Section 3.4 below, abalone become vulnerable to capture at the onset of sexual maturity. The proportion of each age class that is vulnerable to fishing (q) therefore increases monotonically from 0 in immature age classes to 1 in those age classes which contain only sexually mature individuals.

The maximum biomass of a cohort (B_{max}) was calculated using estimates of M and the age-length and length-weight relationships. By incrementing age by small amounts, biomass of a cohort was calculated as

$$B_t = N_t \cdot W_t$$

and B_{max} was determined as the maximum value of B_t .

To conduct the YPR analyses, both F and size at first capture (l_C) were varied incrementally.

2.2.7 Egg per recruit

Egg-per-recruit (EPR) analyses were carried out to examine the proportion of the egg production conserved, relative to that of the unfished stock, at different levels of fishing mortality (F) and minimum size limit (l_C).

Data requirements for the EPR analyses were the same as those for YPR analysis, plus the length-fecundity relationship: fecundity = $a \cdot \text{length}^b$. The parameters of the logistic maturation curve (Equation 2) were used as both the selection coefficient (as described above) and as the maturation coefficient. It is assumed that spawning occurs once per year and that all eggs are released.

Because only the sexually mature abalone (defined as those with visible gonad, not necessarily in ripe condition) within a size or age class will contribute to egg production of that class, the fecundity of an age class is calculated as the product of the number of animals within the age class and the proportion of that age class which is mature times the fecundity of an animal within that age class; *viz.*,

$$\text{fecundity}_t = N_t \cdot q_t \cdot E_t.$$

Similarly, as for YPR analysis, fishing mortality on an age class is modified by the proportion of that age class which is vulnerable to capture, which is the sexually mature fraction of the class. Thus,

$$N_t = N_{t-1} \cdot e^{-(F \cdot q_{t-1} + M)}.$$

EPR was then calculated as $\sum_{t=t_R}^{t_\lambda} N_{t-1} \cdot e^{-(F \cdot q_{t-1} + M)} \cdot E_t \cdot q_t$

and expressed as a percentage of the egg production in the absence of fishing (i.e. $Z = M$):

$$\frac{\sum_{t=t_R}^{t_\lambda} N_{t-1} \cdot e^{-(F \cdot q_{t-1} + M)} \cdot E_t \cdot q_t}{\sum_{t=t_R}^{t_\lambda} N_{t-1} \cdot e^{-M} \cdot E_t \cdot q_t}.$$

3 RESULTS

3.1 Morphometrics

The relationship between shell length and whole weight at each of the sites is shown in Fig. 11 and Table 1. The relationship between shell length and shucked weight of abalone is shown in Fig. 12 and Table 2. Major differences exist between the five sites for both relationships.

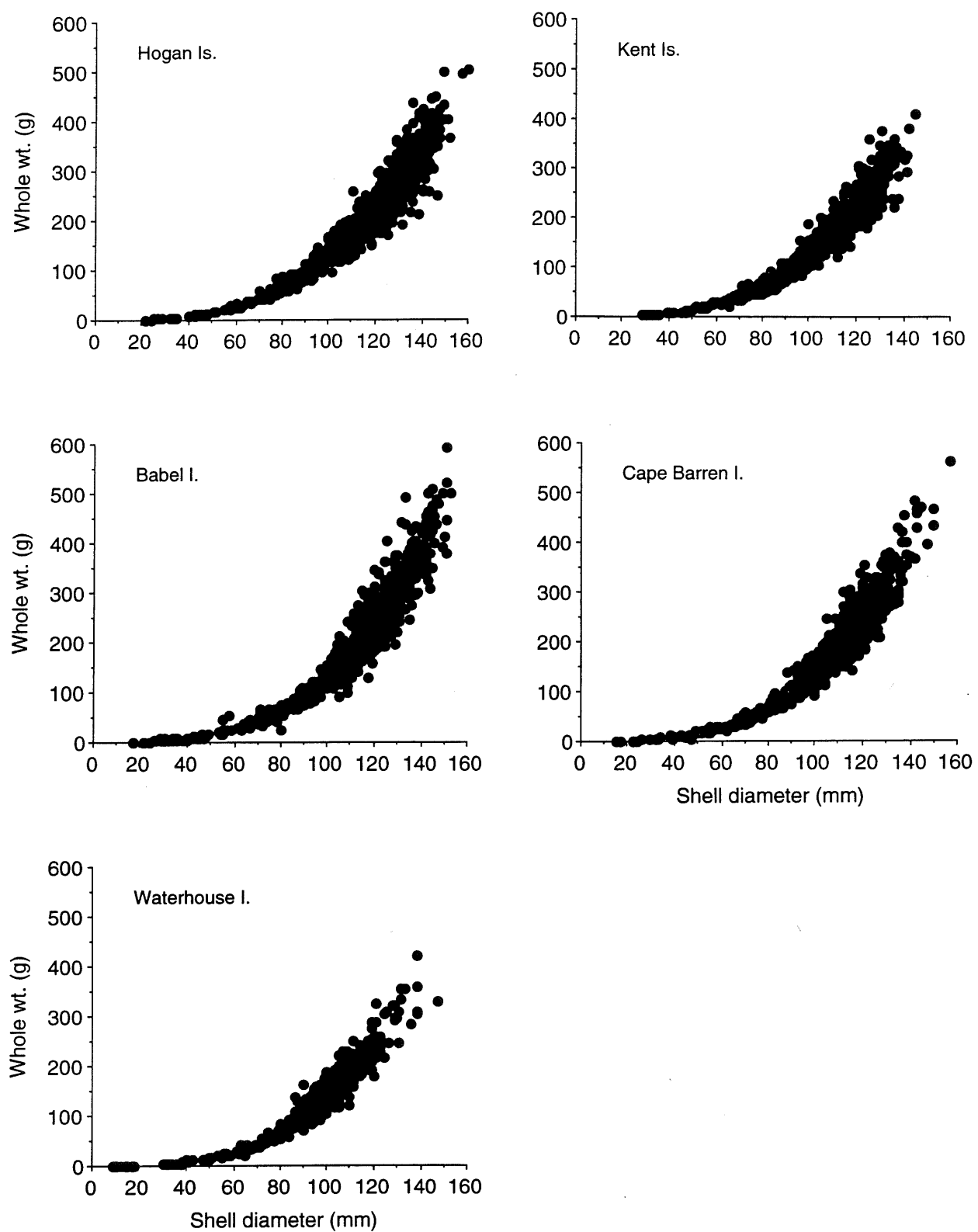


Figure 11. Relationship between shell length and whole weight for *Haliotis rubra* at the five Bass Strait sites.

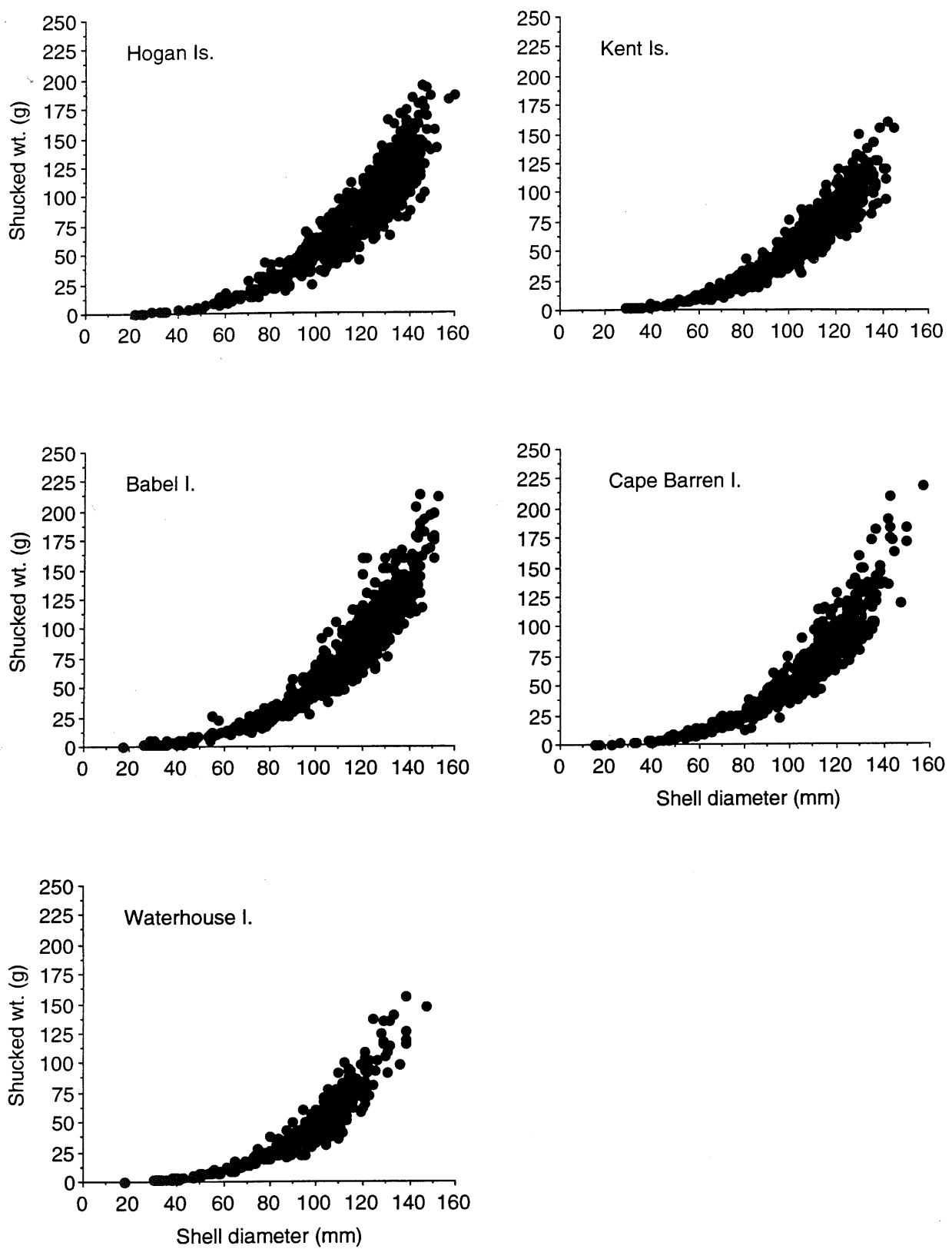


Figure 12. Relationship between shell length and shucked weight for *Haliotis rubra* at the five Bass Strait sites.

Table 1. Relationship between shell length and whole weight of *Haliotis rubra* at the five Bass Strait sites. a and b are constants in the equation whole wt. = $a \cdot (\text{shell length})^b$. 95% confidence limits for b are also given. r^2 = coefficient of determination; n = sample size.

Site	a	b	95% C.L.(b)		r^2	n
			lower	upper		
Hogan Is.	0.0001495	2.962	2.932	2.993	0.971	1097
Kent Is.	0.0000831	3.087	3.057	3.117	0.974	1069
Babel I.	0.0001083	3.040	3.009	3.072	0.973	1015
C. Barren I.	0.0000773	3.122	3.091	3.156	0.976	867
Waterhouse I.	0.0000888	3.095	3.063	3.127	0.983	633

Table 2. Relationship between shell length and shucked weight of *Haliotis rubra* at the five Bass Strait sites. a and b are constants in the equation shucked wt. = $a \cdot (\text{shell length})^b$. 95% confidence limits of b are also given. r^2 = coefficient of determination; n = sample size.

Site	a	b	95% C.L.(b)		r^2	n
			lower	upper		
Hogan Is.	0.0000698	2.928	2.882	2.974	0.936	1087
Kent Is.	0.0000484	2.996	2.956	3.035	0.954	1064
Babel I.	0.0000886	2.882	2.845	2.919	0.959	1011
C. Barren I.	0.0000407	3.045	3.006	3.084	0.965	856
Waterhouse I.	0.0000287	3.104	3.057	3.150	0.965	625

3.2 Age and growth

The proportion of abalone in each sample that could be aged (*i.e.*, for which growth rings could be counted clearly) ranged from 33.0 percent for the Kent Island sample to 47.6 percent at the Waterhouse Island sites (Table 3). The size composition of the ageable and unageable fractions of each population are shown in Fig. 13. Inability to age a shell was because of either physical abrasion of the spire or extensive boring of the shell by polychaetes or sponges.

The relationship between shell size and clarity of growth rings was then examined. The anticipated decline with increasing size of the proportion ageable was observed only for the Hogan population (Fig. 14); for the Kent, Babel and Waterhouse populations, the opposite was found (regression slope greater than 0: $p < 0.05$). There was no detectable trend for the Cape Barren Island population.

Table 3. Miscellaneous statistics for *Haliotis rubra* at the five Bass Strait sites.

Site	Site no.	Sample size	Number of cryptics: non-cryptics ¹	Number of females:males: immature:parasitised ¹	Number of ageable: unageable ¹
Hogan Is.	1	408			
	3	206			
	4	417			
	5	79			
	all	1110	113: 997	528: 479: 97: 6	414: 696
Kent Is.	1	601			
	2	261			
	3	149			
	5	67			
	all	1078	368: 215	473: 148: 444: 5	356: 722
Babel I.	1	599			
	2	422			
	all	1021	165: 505	439: 478: 102: 1	414: 607
C. Barren I.	1	415			
	2	362			
	3	89			
	all	909	267: 445	382: 402: 120: 2	346: 563
Waterhouse I.	1	348			
	2	38			
	3	143			
	4	69			
	5	38			
	all	636	172: 395	242: 320: 70: 1	303: 333

¹These do not necessarily sum to the total sample size, because of difficulty assigning individuals to one category or another, or to missing data.

The relationship between shell length and number of major shell growth rings of *Haliotis rubra* at each of the five Bass Strait sites is shown in Fig. 15 (top row of graphs). There was wide variation in length at age at all five sites, as illustrated for the Babel Island site in Fig. 16. The age and length compositions of each population are shown in Figs. 17 and 18 respectively.

Values of both the Gompertz and von Bertalanffy growth parameters are shown in Table 4, derived using a shell layer deposition rate of one per year. For two growth rings per year, K is doubled and t_0 is halved relative to the estimates obtained using one growth ring per year; L_∞ does not change. L_∞ ranged from 112.6 mm at Waterhouse Island to 130.4 mm at Babel Island (Table 4). The estimate of L_∞ calculated from the Gompertz analysis is invariably lower than the von Bertalanffy estimate. The high t_0 values shown (2.4 to 3.5 yr for one growth ring per year) indicate the considerable time after ‘birth’ that the growth rate is maximal (the point of inflection on the curve), after which the von Bertalanffy growth function may be fitted to the data.

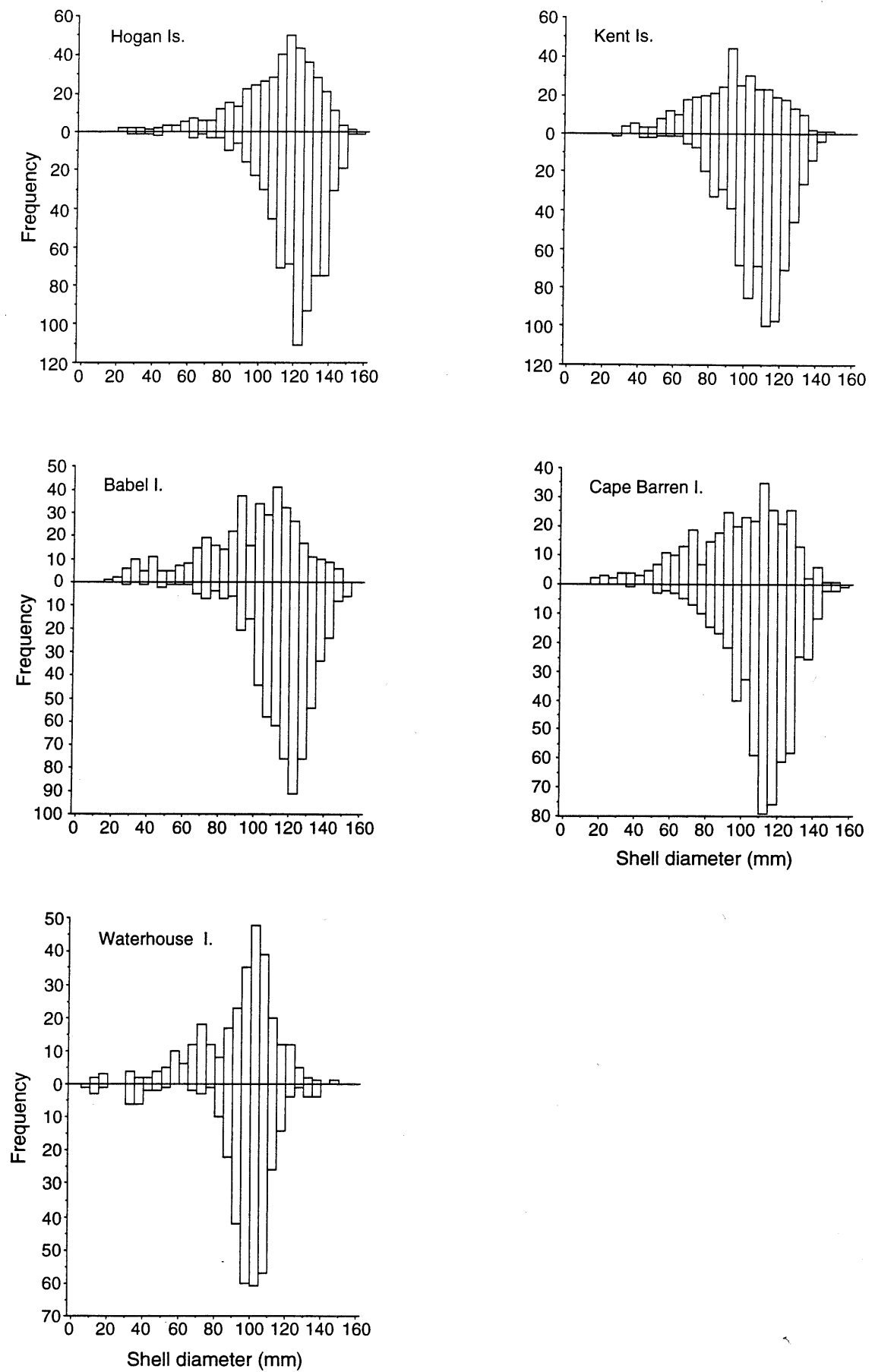


Figure 13. Length composition of ageable and unageable *Haliotis rubra* from each of the Bass Strait sites.
Ageable above the x-axis, unageable below the x-axis.

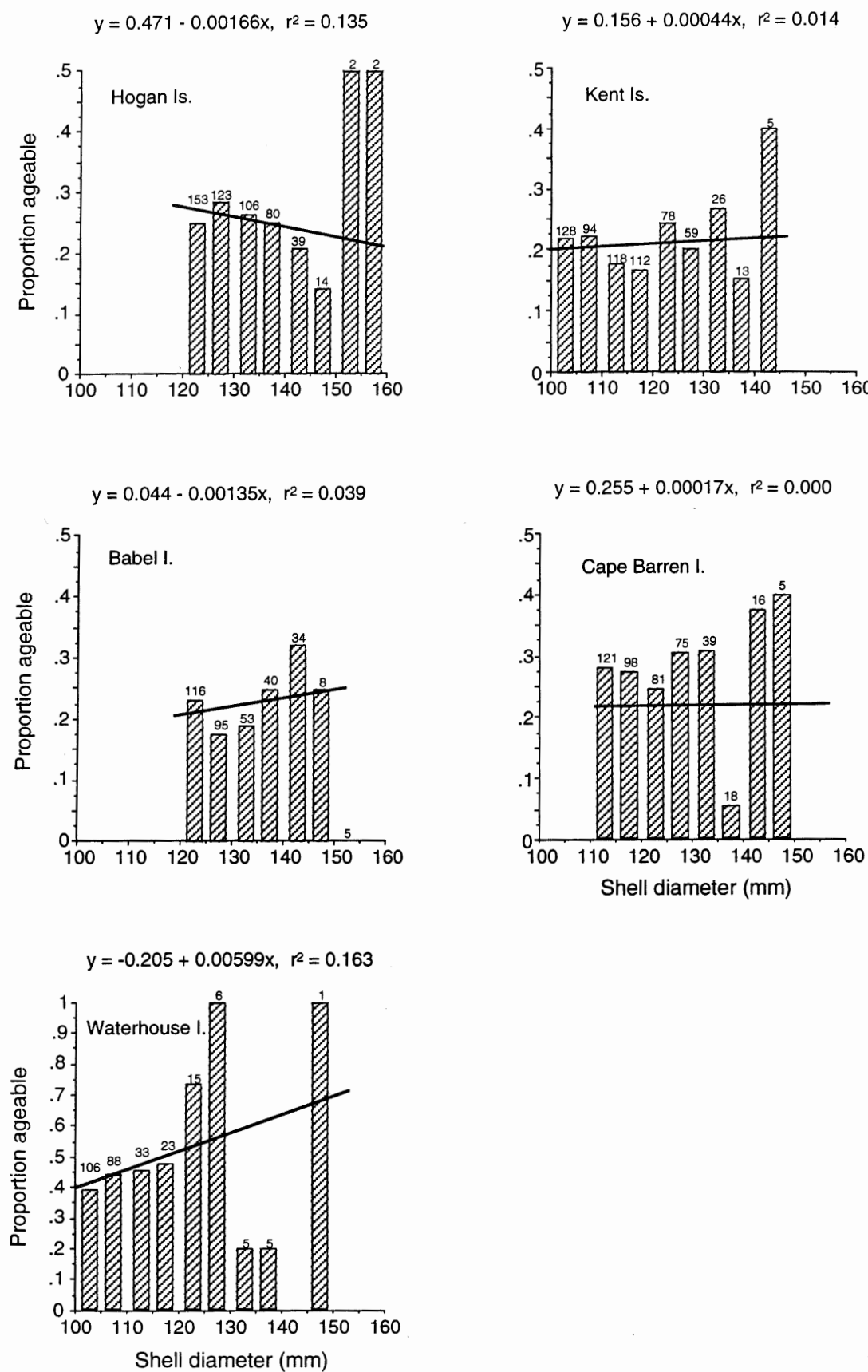


Figure 14. The proportion of abalone in each 5-mm length class which could be aged. Only size classes larger than the modal length class (approximately corresponding to the modal age class) were used in the analysis. The regression line was fitted after weighting each proportion by sample size (shown above each bar).

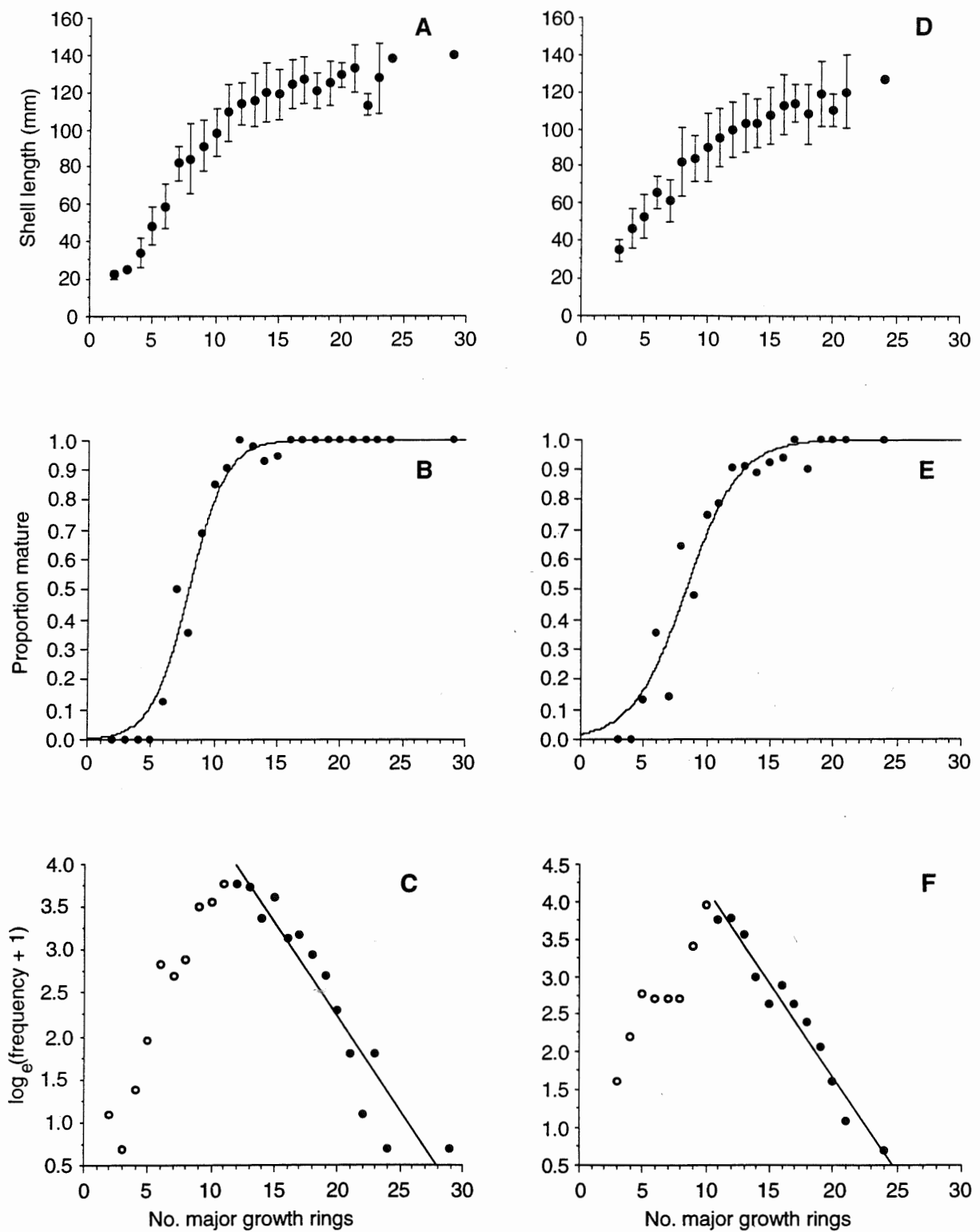


Fig. 15. Growth, maturation and mortality of *Haliotis rubra* from the Hogan Islands (A-C), Kent Islands (D-F), Babel Island (G-I), Cape Barren Island (J-L) and Waterhouse Island (M-O). The number of major shell growth rings is used as the independent variable as a measure of age, since the rate of ring deposition is not known. Rates of growth and total mortality (Z) were then calculated for both one and two growth rings per year. (A,D,G,J,M) 'Age'-length relationship; (B,E,H,K,N) 'Age' at maturity; (C,F,I,L,O) 'Age'-frequency plots from which Z was calculated as $-(\text{slope of the regression line fitted to the solid data points (●)})$. Error bars in A, D, I, J and M are 1 standard deviation.

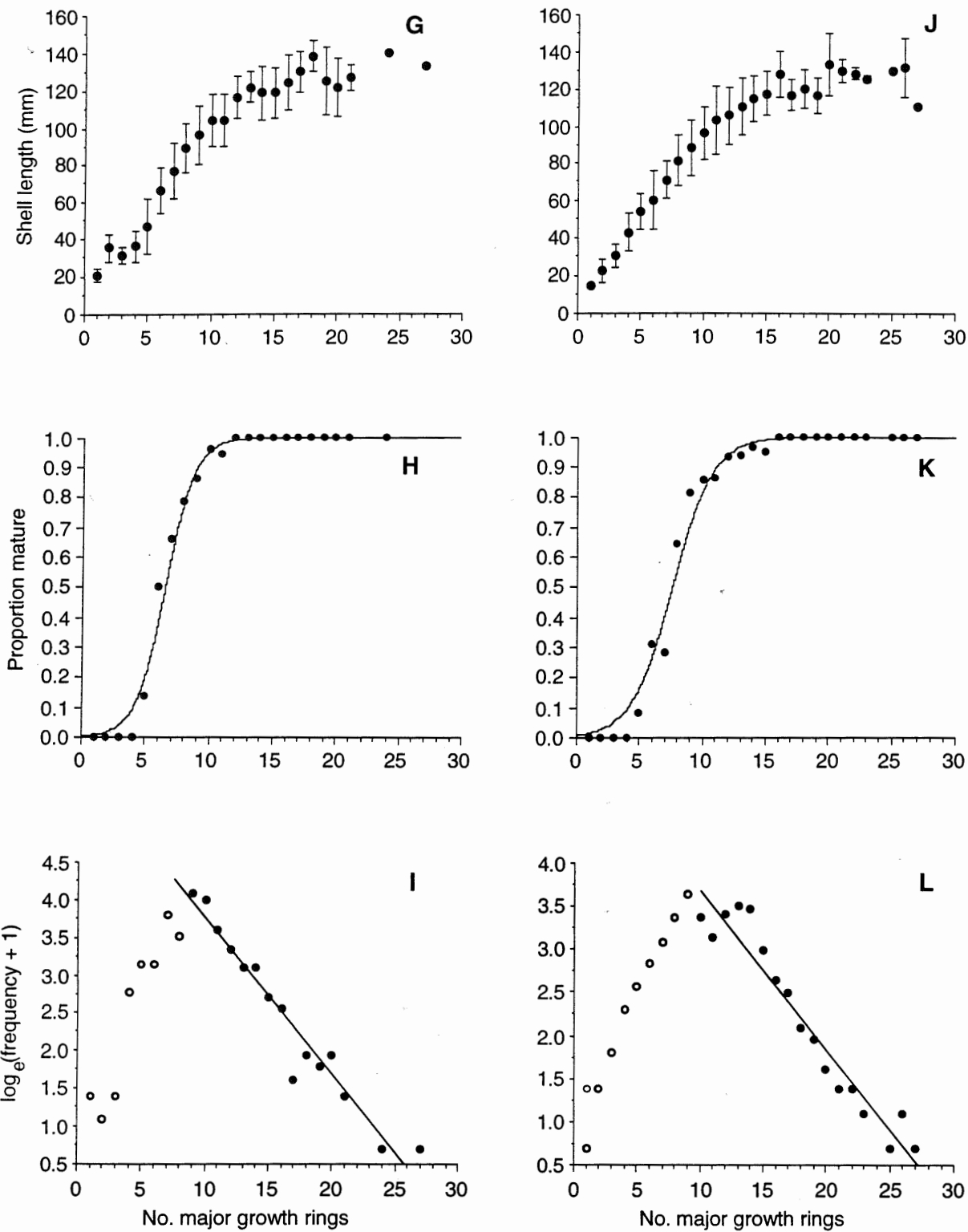


Figure 15 – continued.

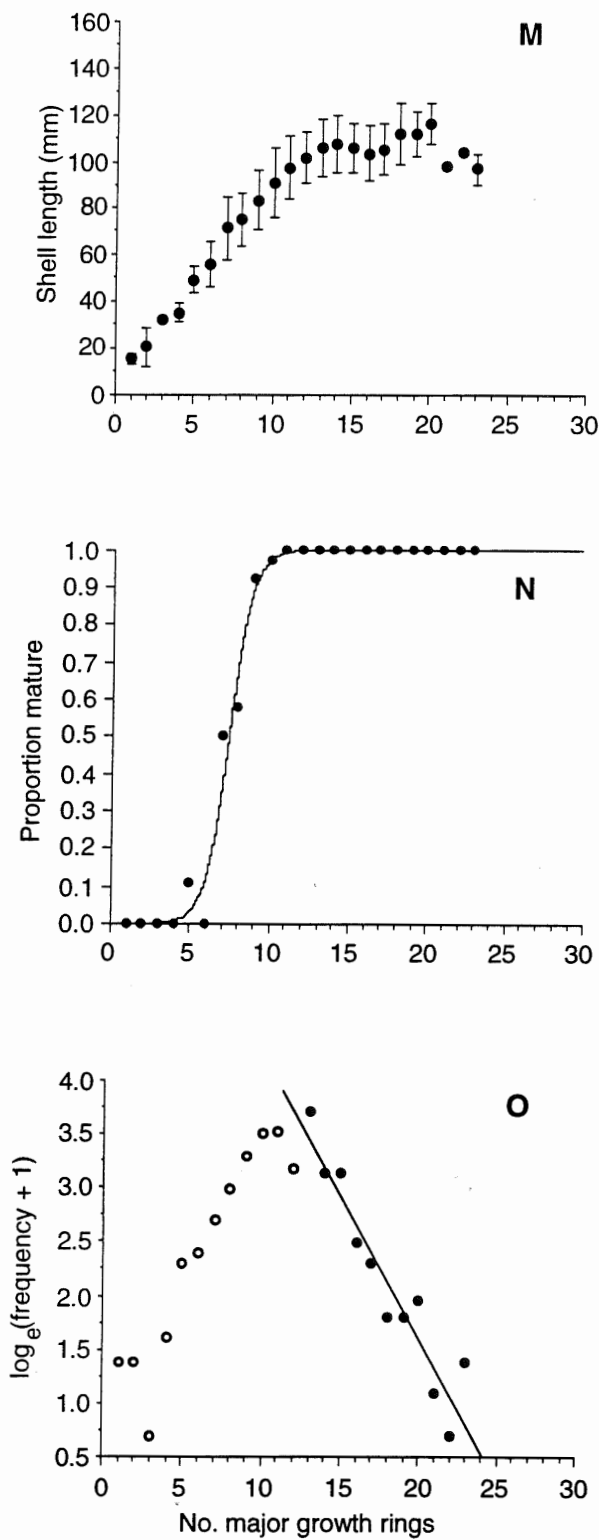


Figure 15 – concluded.

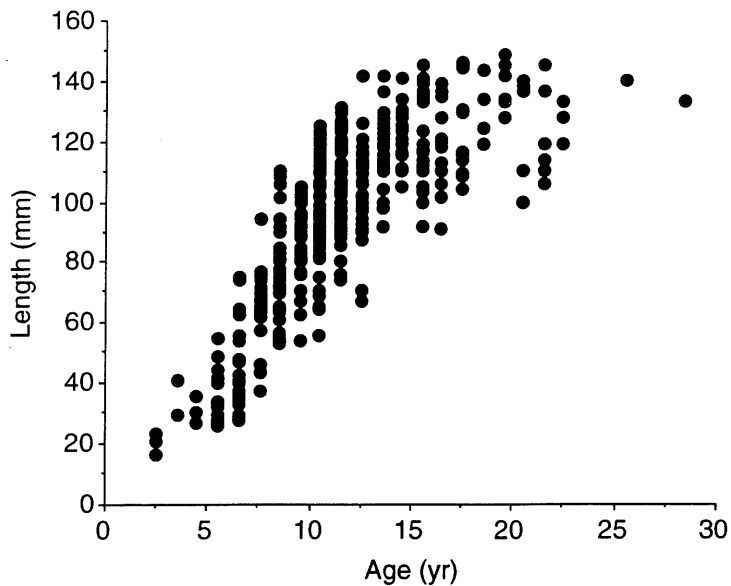


Figure 16. Relationship between age and shell length of *Haliotis rubra* from Babel Island, illustrating the variation in growth rate that exists.

The age-length data for males and females were also analysed separately (Table 4). For these analyses, the age-length data for immature abalone were combined with those of the separate sexes. This was done so that, as far as possible, the entire size range of each sample was included in the analyses. Note, however, that this procedure leads to von Bertalanffy parameter values that correspond more closely to the juvenile data than is the case for the combined data. Because juvenile growth is approximately linear, the effect of having relatively more juveniles in the data is to lower K and to increase L_∞ . The magnitude of the effect depends on the number of males (or females) in the sample analysed. Gompertz analyses, with an extra parameter, are less affected.

Using the von Bertalanffy growth parameters to compare the growth of males and females, the asymptotic length (L_∞) was greater for males than females at four of the five sites, and the Brody growth coefficient (K) was greater for females than males at all sites (Table 4). In other words, females generally have a smaller maximum size, and they grow to their maximum size more rapidly than males. (The von Bertalanffy growth function is used to compare growth between the sexes here, despite the better fit of the Gompertz growth function, because K is easier to interpret than the Gompertz rate parameters G and g .)

Goodness of fit of the age-length data (as measured by the r^2 value) to the growth function reveals that, in 14 of the 15 analyses, the goodness of fit is better for the Gompertz function (Table 4), perhaps because of the sigmoidal form of the age-length data. It can be seen (Table 4) that three of the five comparisons between the sexes by the von Bertalanffy method yielded

estimates of L_∞ that were higher than for the sexes combined; as noted above, this may be attributable to the greater influence of the juvenile data when the data are analysed by sex.

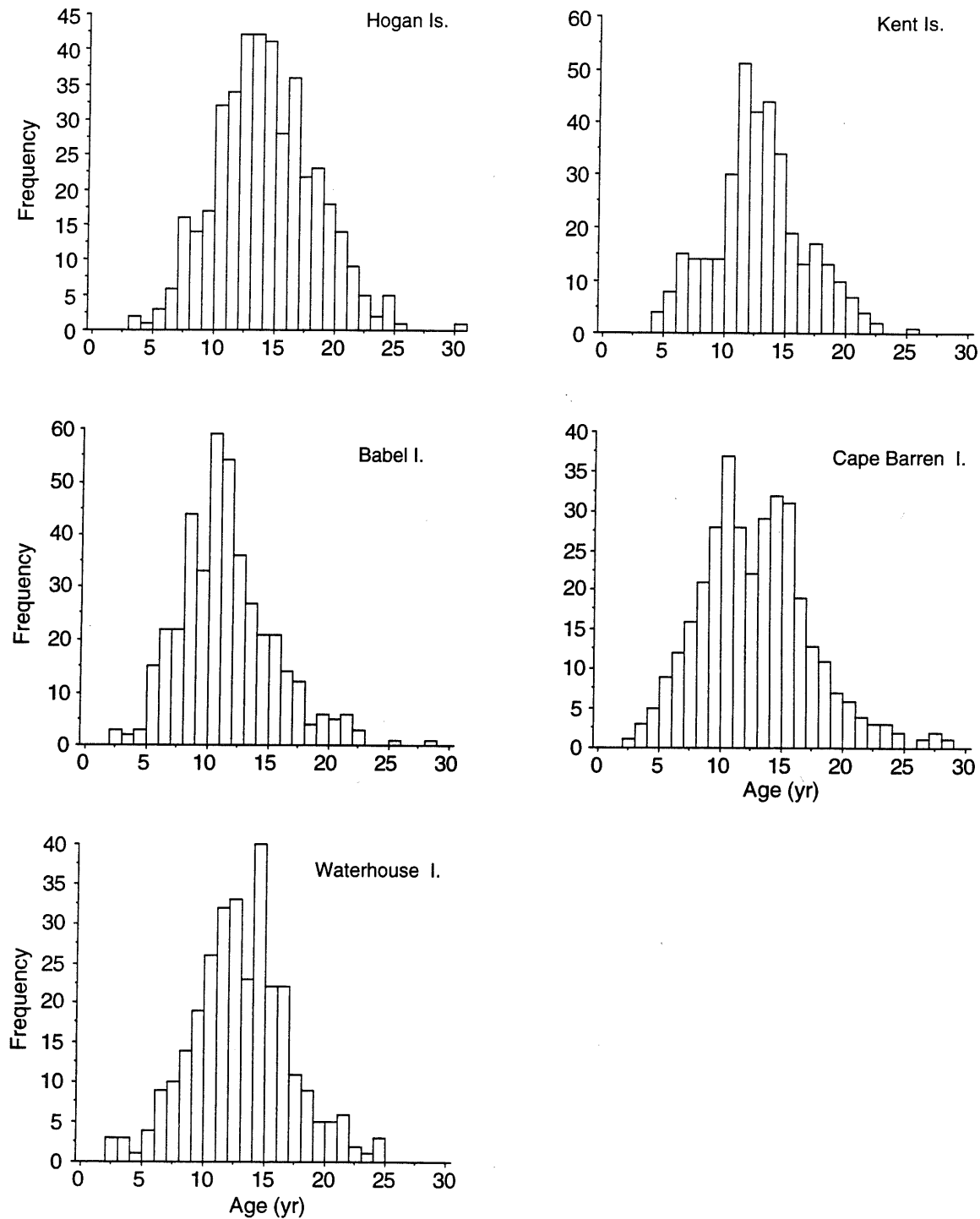


Figure 17. Age composition of *Haliotis rubra* at the five Bass Strait sites.

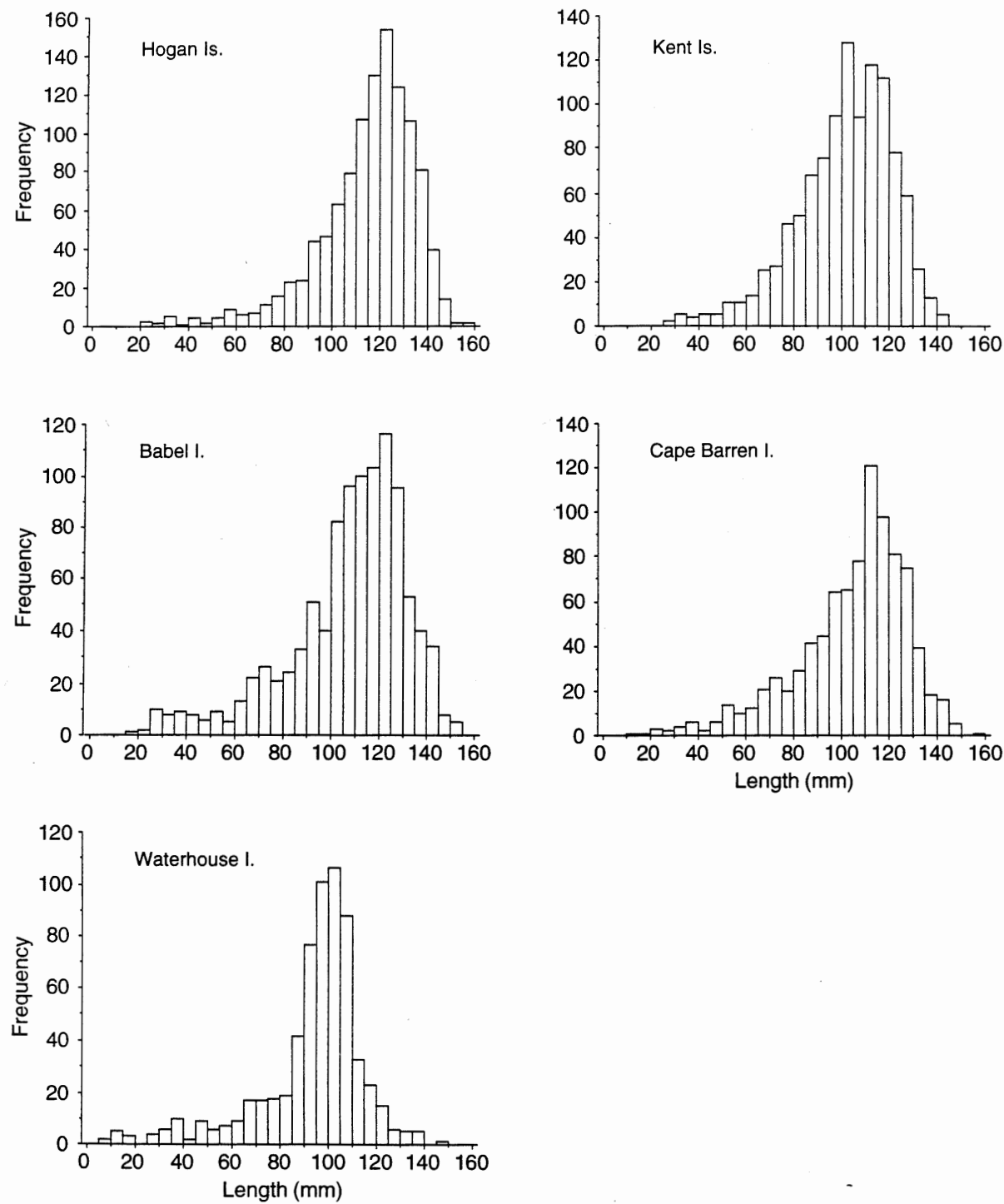


Figure 18. Length composition of *Haliotis rubra* at the five Bass Strait sites.

Table 4. Gompertz and von Bertalanffy growth parameters of *Haliotis rubra* at the five Bass Strait survey sites, assuming one major shell growth ring per year. Samples from sites within each area were combined for these analyses. Analyses were conducted on the separate sexes (fem+imm, male+imm) and the sexes combined. See the text for a description of the growth parameters. fem=female; imm=immature; r^2 = coefficient of determination; n = sample size. L_∞ in mm; K per year; t_0 in years.

Area	Gompertz					von Bertalanffy				n
	l_0	G	g	L_∞	r^2	L_∞	K	t_0	r^2	
Hogan Is.										
all	0.459	5.637	0.273	128.8	0.695	135.7	0.168	3.508	0.686	413
fem+imm	0.487	5.589	0.266	130.3	0.750	138.9	0.156	3.446	0.737	244
male+imm	1.159	4.711	0.246	128.8	0.740	138.6	0.144	3.179	0.735	234
Kent Is.										
all	5.356	3.111	0.207	120.2	0.598	127.0	0.135	2.388	0.596	356
fem+imm	4.461	3.278	0.211	118.3	0.641	126.4	0.132	2.423	0.636	234
male+imm	11.500	2.421	0.154	129.5	0.638	143.4	0.089	1.276	0.639	217
Babel I.										
all	0.542	5.483	0.275	130.4	0.770	146.1	0.136	2.863	0.751	414
fem+imm	0.333	5.982	0.280	131.9	0.803	153.0	0.124	2.832	0.776	245
male+imm	1.345	4.594	0.241	133.0	0.811	155.4	0.110	2.572	0.795	256
Cape Barren I.										
all	2.743	3.852	0.222	129.2	0.767	139.4	0.129	2.634	0.761	344
fem+imm	3.048	3.748	0.216	129.3	0.787	142.4	0.119	2.480	0.781	210
male+imm	4.548	3.374	0.193	132.8	0.797	148.1	0.104	2.258	0.792	218
Waterhouse I.										
all	0.582	5.265	0.281	112.6	0.736	121.6	0.151	2.545	0.714	303
fem+imm	0.623	5.179	0.279	110.6	0.824	121.6	0.139	2.392	0.798	143
male+imm	1.181	4.586	0.254	115.9	0.783	128.5	0.129	2.369	0.766	207

The age-length data were further analysed to examine the relationship between sexual condition (whether immature or mature) and size within individual age classes. Clearly, only those age classes comprising both immature and mature animals could be used in this analysis. Without exception, the mean size of the sexually mature fraction of an age class is greater than that of the immature fraction (Fig. 19). This pattern has been found, without exception, at about 20 sites around Tasmania (unpublished results).

This result, which was not anticipated, provides circumstantial evidence that the relationship between number of growth rings in the shell and age is a close one; it is difficult to imagine that such a result could have been obtained in the absence of such a relationship. There is, however, insufficient evidence from this result alone to determine whether the rate of shell layer deposition is one per year, or several.

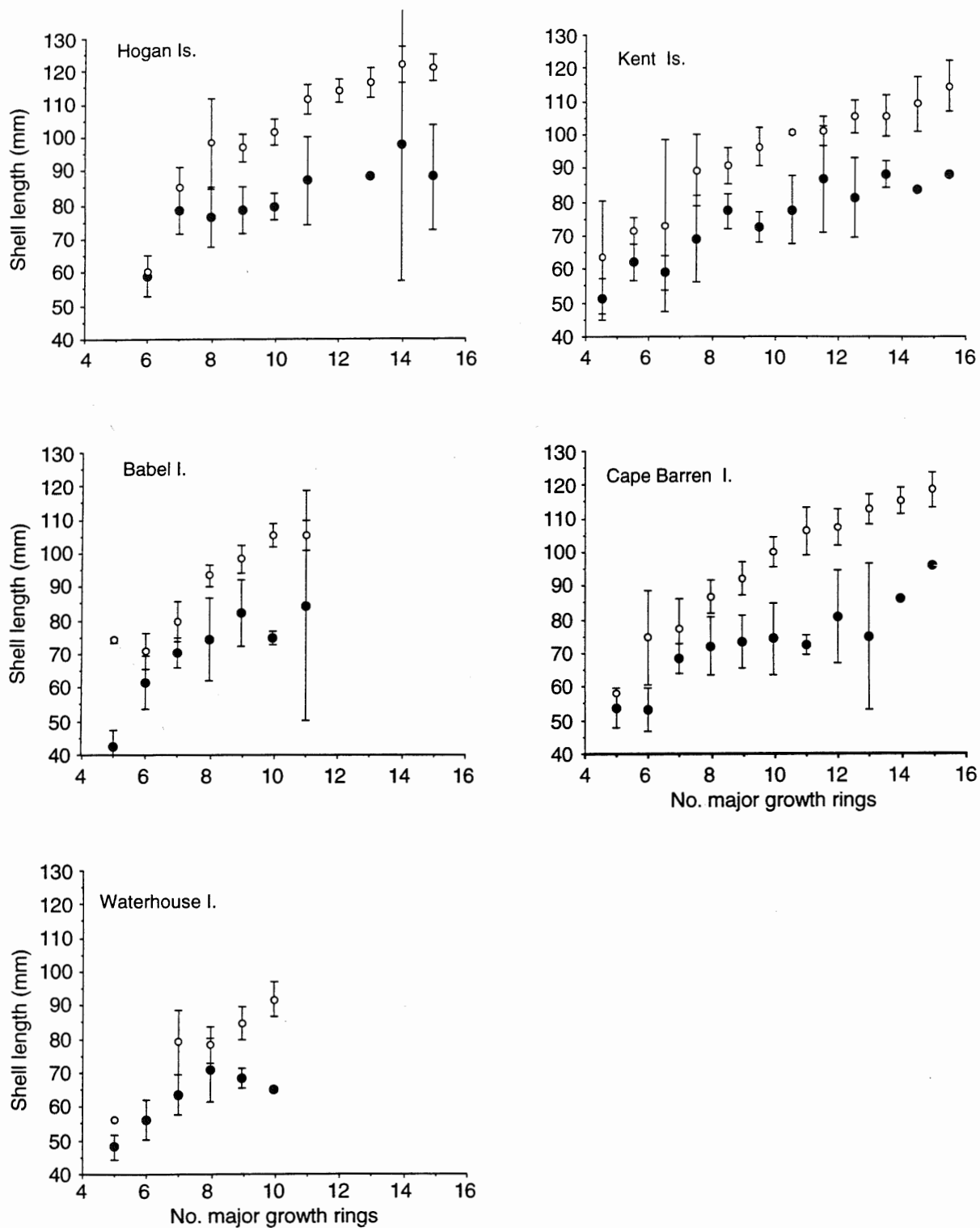


Figure 19. Mean lengths of immature and mature *Haliotis rubra* within individual growth ring classes.
Within a ring class, mature abalone are larger than immature abalone. ● Immature ○ Mature. Error bars are 95% confidence limits.

3.3 Sexual maturation and fecundity

3.3.1 Onset of sexual maturity

The process of sexual maturation with age follows a similar pattern in each of the five areas: onset of maturity begins in abalone aged between five and seven years (assuming one growth ring per year), with an increasing proportion of successively older year classes being mature (Fig. 15, middle row of graphs). Maturation of each population occurs over several years, so that it is only in year classes 13 to 15 and older that all animals are sexually mature. Age at 50 percent maturity ranges from 8.0 to 9.9 years (Table 5), with the rate of transition from immature to mature (measured by the parameter b of the logistic equation) highest at Waterhouse Island ($b=1.379$) and lowest in the Kent group ($b=0.628$).

The process of sexual maturation with size varies between sites according to growth rates: gonad development is first seen in 45-50 mm abalone at Waterhouse Island (where stunting is most pronounced) to 60-65 mm at the Hogan Islands (Fig. 20). Full sexual maturity occurs at c. 90 mm (Waterhouse Island) through to c. 120 mm (Hogan Islands). Size at 50 per cent maturity ranges from 65.3 to 82.6 mm (Table 5).

Table 5. Rates of onset of sexual maturity by length and by age of *Haliotis rubra* at each of the five Bass Strait sites. a and b are the parameters of the logistic function shown in Equation 2. $L_{0.5}$ and $D_{0.5}$ are the length and age, respectively, at which *H. rubra* is 50 percent sexually mature.

Site	Length				Age					
			95% C.L. ($L_{0.5}$)				95% C.L. ($D_{0.5}$)			
	a	b	$L_{0.5}$	lower	upper	a	b	$D_{0.5}$	lower	upper
Hogan Is.	-12.770	0.155	82.6	79.8	85.1	-6.558	0.692	9.5	8.8	10.0
Kent Is.	-8.073	0.110	73.6	70.7	76.0	-4.750	0.482	9.9	9.1	10.5
Babel I.	-8.517	0.123	69.0	65.6	72.0	-7.082	0.880	8.0	7.6	8.4
Cape Barren I.	-10.960	0.145	75.6	73.0	78.0	-5.707	0.628	9.1	8.5	9.6
Waterhouse I.	-11.120	0.170	65.3	61.8	68.3	-12.290	1.379	8.9	8.4	9.3

3.3.2 Fecundity

The relationship between age and fecundity (measured as gonad cross-sectional area) is poor (Fig. 21). By contrast, the relationship between length and fecundity (Fig. 22) is much closer, although still wide. The values of a and b in the equation

$$\text{Fecundity} = a \cdot (\text{Length})^b \quad (3)$$

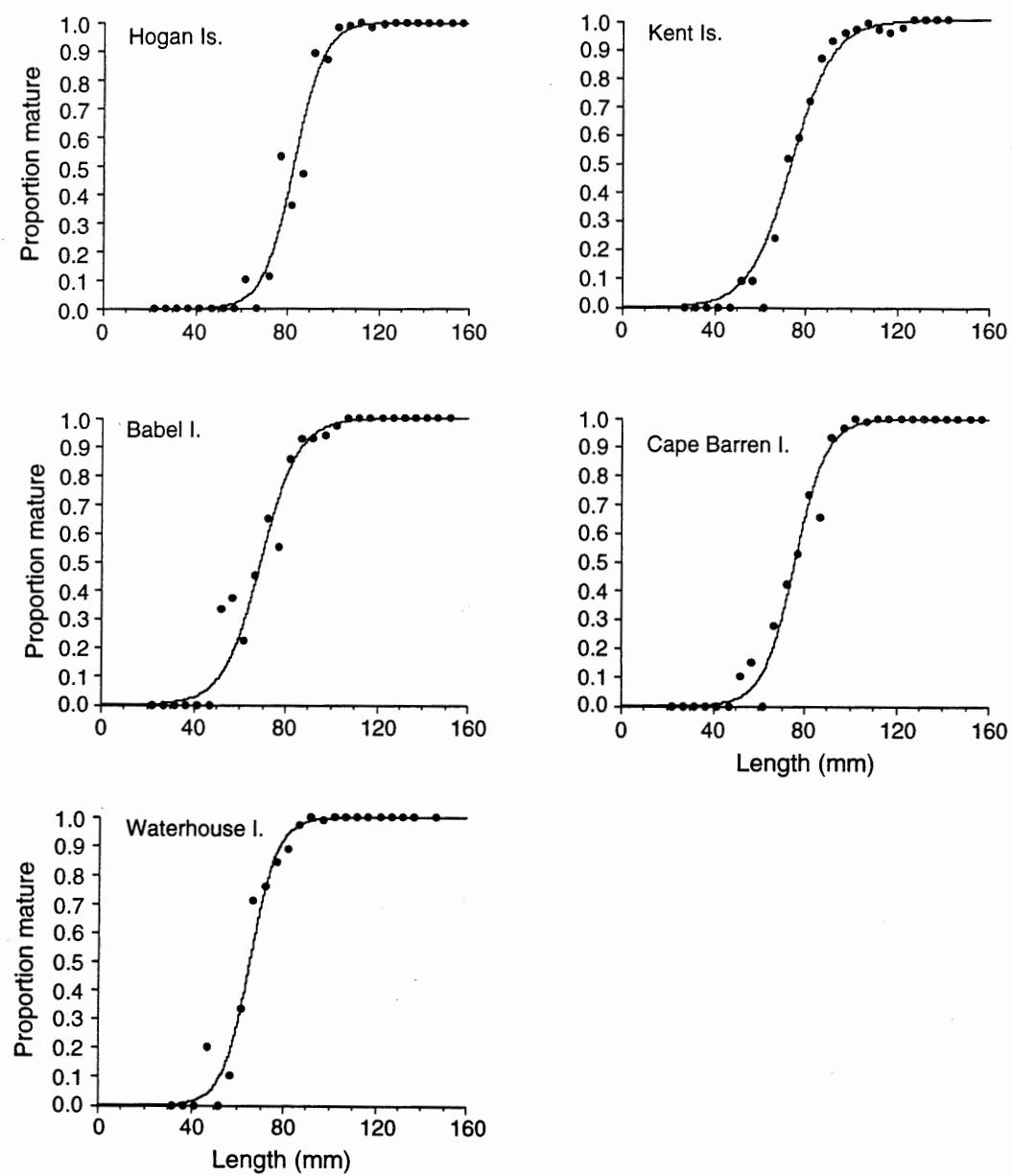


Figure 20. Rates of maturation by length of *Haliotis rubra* at the five Bass Strait sites.

show that fecundity increases exponentially with length (Table 6). At four of the five sites, the rate of increase of fecundity with length was allometric ($b>3$).

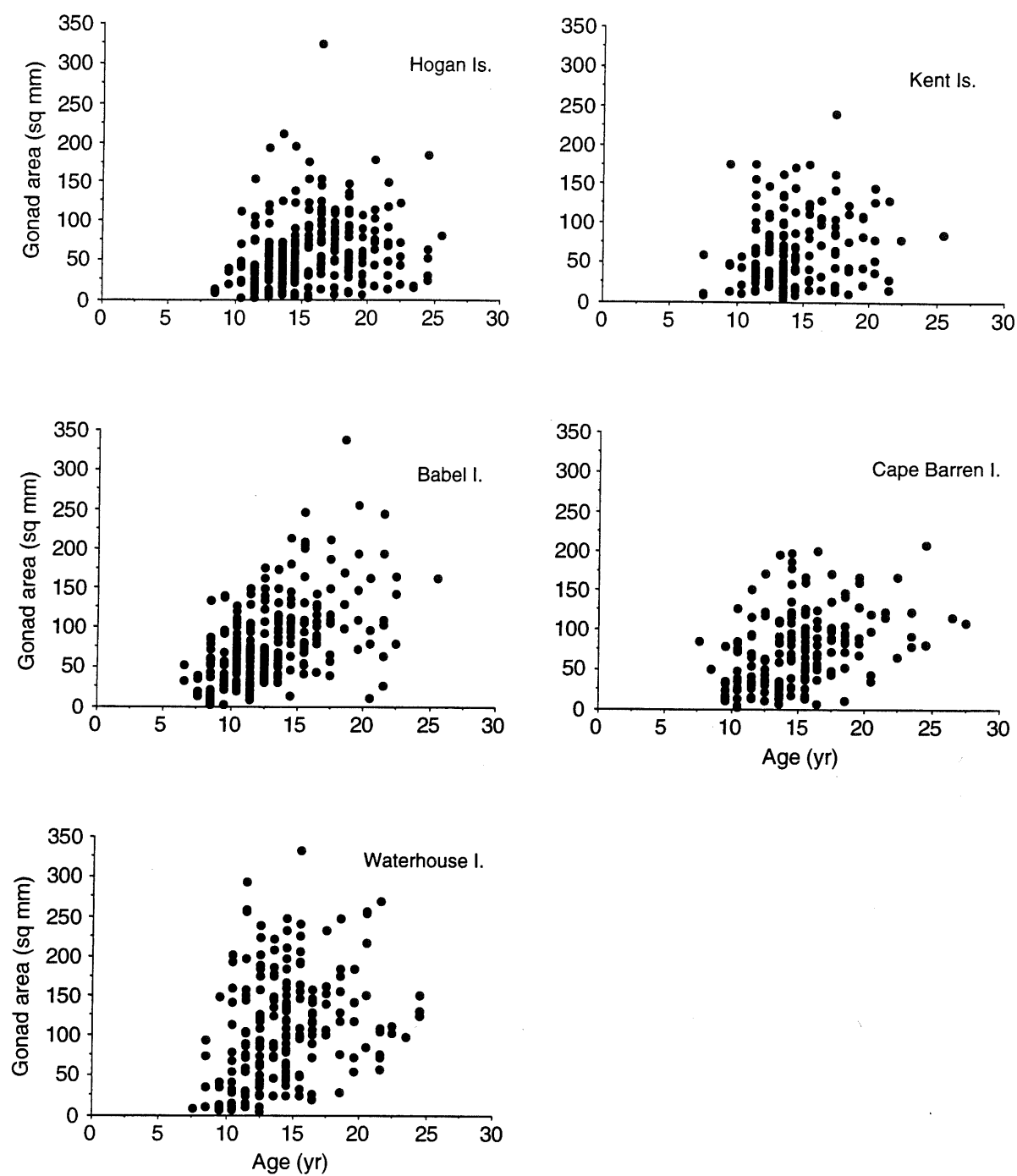


Figure 21. Relationship between age and fecundity (measured as cross-sectional area of the conical appendage of the gonad) of *Haliotis rubra* at the five Bass Strait sites.

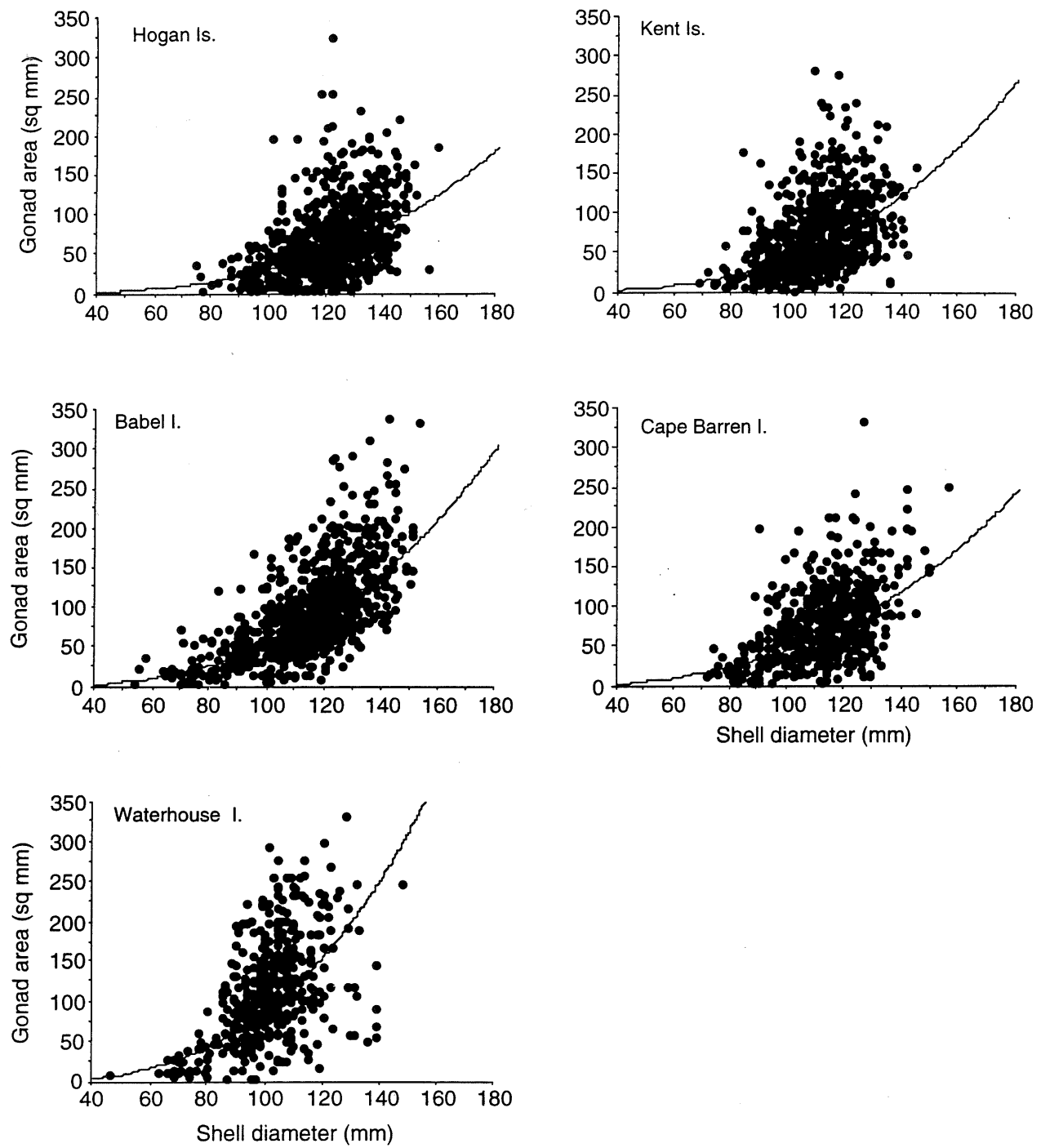


Figure 22. Relationship between length and fecundity (measured as cross-sectional area of the conical appendage of the gonad) of *Haliotis rubra* at the five Bass Strait sites. Fitted power curves are shown; parameter values for these curves are given in Table 6.

Table 6. Relationship between shell length and fecundity (measured as cross-sectional gonad area) of *Haliotis rubra* at the five Bass Strait sites. a and b are constants in the equation fecundity = $a \cdot (\text{shell length})^b$. 95% confidence limits for b are also given. r^2 = coefficient of determination; n = sample size.

Site	a	b	95% C.L.(b)		r^2	n
			lower	upper		
Hogan Is.	0.0000116	3.196	2.778	3.613	0.218	810
Kent Is.	0.0000163	3.207	2.793	3.622	0.262	653
Babel I.	0.0000523	3.004	2.794	3.215	0.492	814
C. Barren I.	0.0000750	2.894	2.504	3.284	0.265	590
Waterhouse I.	0.0000385	3.186	2.761	3.611	0.329	445

The relationship between whole weight and fecundity (measured as gonad cross-sectional area) is shown in Fig. 23 and Table 7. The relationship was linear at all five sites (exponent of the power curve = 1).

The relationships between age, size and fecundity were then examined further in order to determine whether age or size is the more important determinant of fecundity. The Babel Island site is used to illustrate the procedure and the findings. The same pattern was found at the other four sites. The procedure used is as follows.

The residuals about the non-linear least squares regression line fitted to the age-length data using the Gompertz growth function were obtained using FISHPARM (Prager *et al.* 1987), with length as the dependent variable. The residuals about the linear least squares regression line fitted to the fecundity-length data [both $\log_e(x+1)$ -transformed] were then obtained, with fecundity as the dependent variable. Fecundity was then regressed against age and the residuals were computed.

The question that was then addressed is: *Do abalone which are large for their age have smaller gonads than older abalone of the same size?* If the answer to this question is 'yes', then it may be concluded that age is an important determinant of fecundity. When this question was examined by plotting the residuals of the length-fecundity regression against the residuals of the age-length regression, the slope of the regression line did not differ significantly from zero (Fig. 24A; $p>0.05$). It is therefore concluded that the length-fecundity relationship is not confounded by age-related effects, and abalone of a given size within a site will have a fecundity that is independent of age.

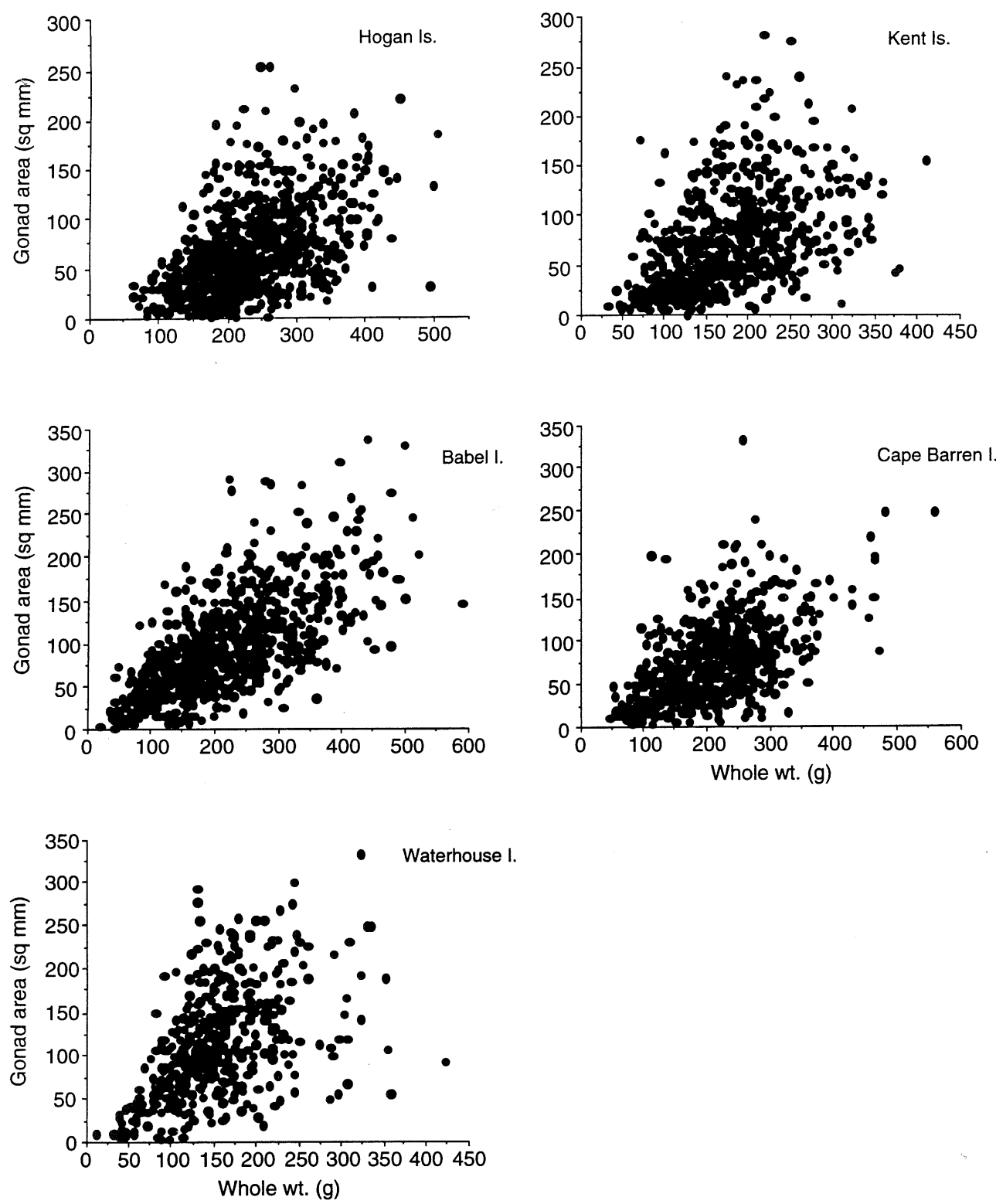


Figure 23. Relationship between whole weight and fecundity (measured as gonad cross-sectional area) for *Haliotis rubra* at the five Bass Strait sites.

Table 7. Relationship between whole weight and fecundity (measured as cross-sectional gonad area) of *Haliotis rubra* at the five Bass Strait sites. a and b are constants in the equation fecundity = a + b .(whole weight). 95% confidence limits for b are also given. r^2 = coefficient of determination; n = sample size.

Site	a	b	95% C.L.(b)		r^2	n
			lower	upper		
Hogan Is.	2.945	0.273	0.237	0.309	0.217	809
Kent Is.	12.701	0.341	0.291	0.392	0.214	653
Babel I.	12.160	0.381	0.353	0.410	0.464	809
C. Barren I.	12.053	0.314	0.274	0.354	0.289	587
Waterhouse I.	36.744	0.503	0.419	0.588	0.236	445

When the residuals of the age-fecundity regression were then plotted against the residuals of the age-length regression, a significant positive slope to the regression line was obtained (Fig. 24B: slope = 1.784; $p < 0.05$). Thus, fast-growing abalone (i.e. those that are large for their age) have bigger gonads (are more fecund) than slow-growing animals of the same age; in other words, fecundity is dependent on abalone size.

These results show that fecundity is size-dependent rather than age-dependent. The poor age-fecundity relationship (Fig. 21) may then be explained by the fact that (i) fecundity is determined primarily by size (bigger abalone have bigger gonads, regardless of their age), and (ii) growth rates vary greatly between abalone (Fig. 16) so that, for any given age, the abalone are of a considerable range of sizes.

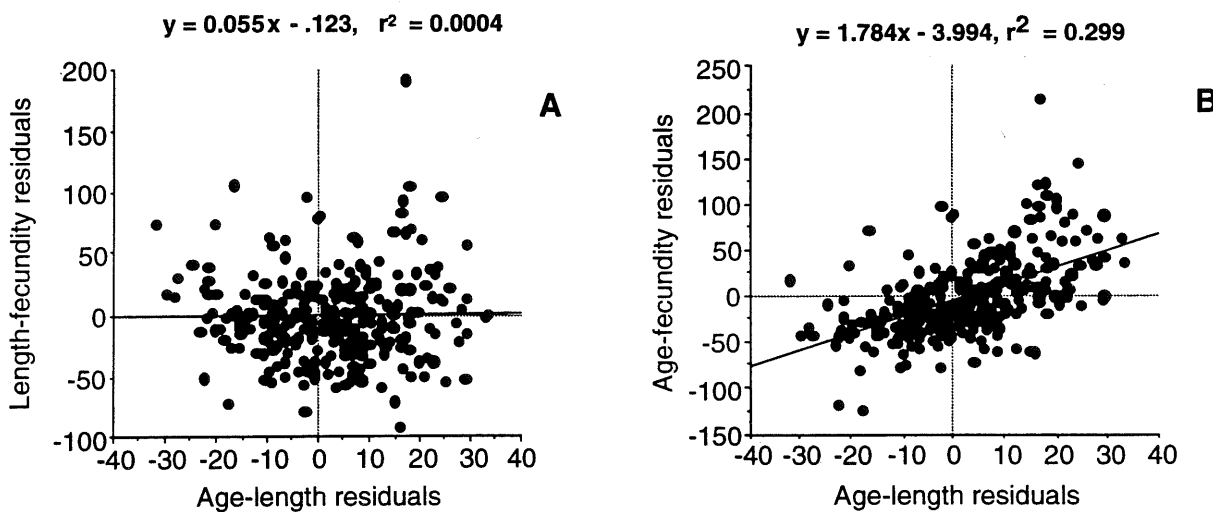


Figure 24. An investigation by residuals analysis of whether fecundity is more closely related to age or to size for *Haliotis rubra*, illustrated by the Babel Island population. The same pattern was seen at the other four Bass Strait sites. (A) Determination of whether fecundity is closely related to age. If it were, abalone that are large for their age should have smaller gonads than older abalone of the same size (and vice versa), and the slope of the regression line should be negative. This was not so (slope = 0). (B) Abalone that are large for their age are also fecund for their age (and vice versa), illustrating that fecundity is independent of age and closely related to size.

3.4 Cryptic and emergent abalone

The length and age compositions of the cryptic and emergent fractions of the population samples collected at each site are shown in Figs. 25 and 26 respectively. At all sites cryptic abalone are both smaller and younger than the emergent fraction.

It is important to note that the age at which the abalone become fully recruited to the fishery (Fig. 15, bottom row) closely coincides with the age at which 90 to 100 percent of the population has reached sexual maturity, except for the Waterhouse Island animals (Fig. 15, middle row). At Waterhouse Island full sexual maturity occurred slightly earlier than full recruitment. Even in the absence of analyses comparing the age and maturity of cryptic and non-cryptic abalone, this provides support for the hypothesis that *Haliotis rubra* emerges from the sub-boulder or crevice habitat at the onset of sexual maturity.

The hypothesis that *Haliotis rubra* emerge at the onset of sexual maturity was then examined directly. If strictly true, all cryptic abalone should be sexually immature and all emergent abalone sexually mature. The proportion mature of the cryptic and emergent fractions of the population samples were examined in 5-mm increments (Fig. 27). It is apparent from this figure that the hypothesis is not supported unequivocally: at all sites a substantial proportion of the cryptic abalone are sexually mature, and this proportion increases with increasing size. Only size classes which include sexually immature abalone are shown in Fig. 27; for larger sizes the proportion sexually mature is 1, whether cryptic or emergent. The proportion values used to construct Fig. 27 do not show that the number of large cryptic abalone is very small relative to the number of large emergent abalone; this can be seen by reference to Fig. 25.

3.5 Mortality

The catch curves used to calculate instantaneous total mortality (Z) for each of the five sites are shown in Fig. 15 (bottom row). The estimated instantaneous total mortalities at the four sites range from 0.185 at Cape Barren Island to 0.265 at Waterhouse Island (if one growth ring per year) or 0.370 to 0.529 (if two rings per year) (Table 8). Corresponding annual survival rates are also shown.

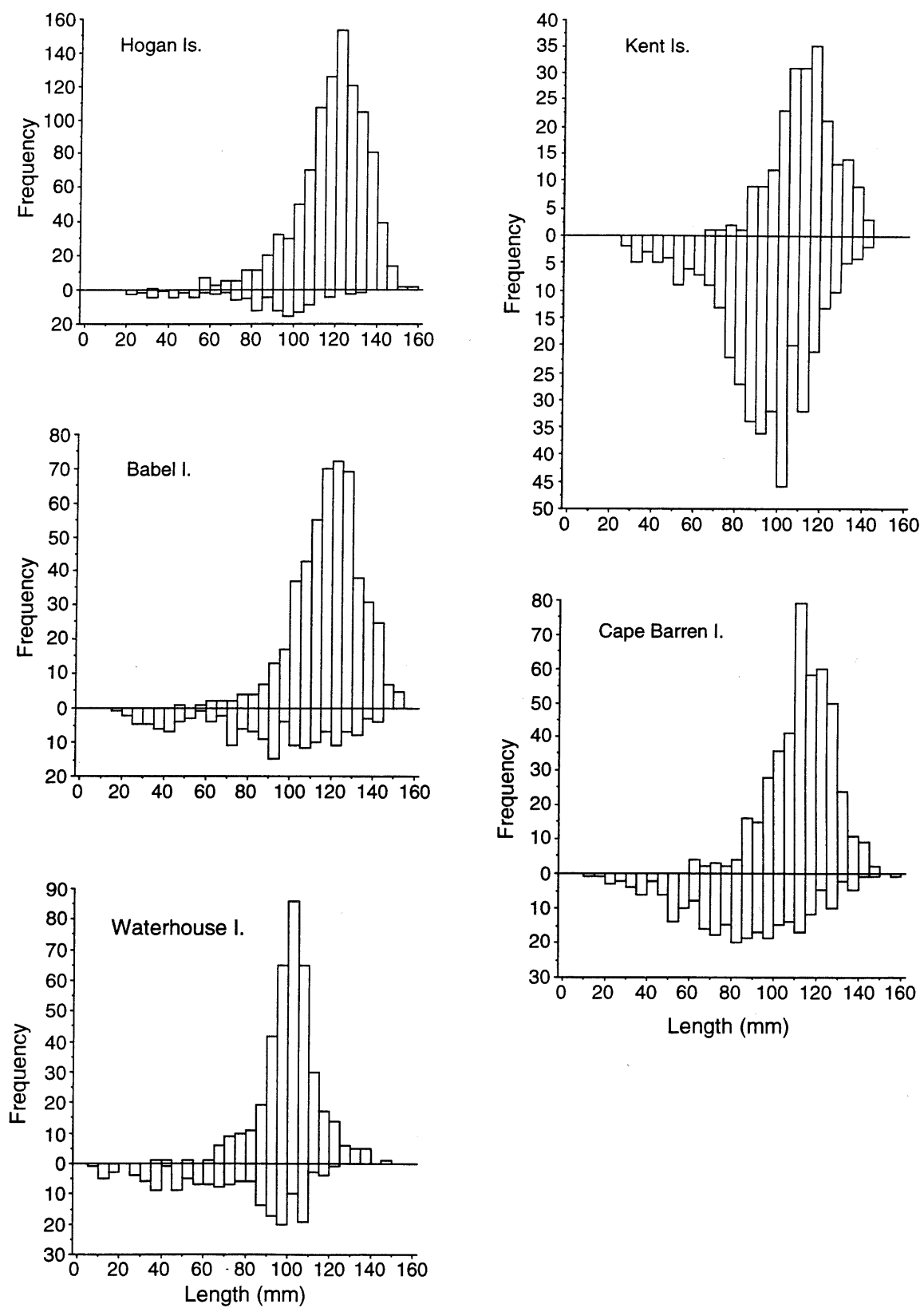


Figure 25. Length composition of cryptic and emergent blacklip abalone (*Haliotis rubra*) at each of the Bass Strait sites. Emergent abalone above the x -axis, cryptic abalone below the x -axis.

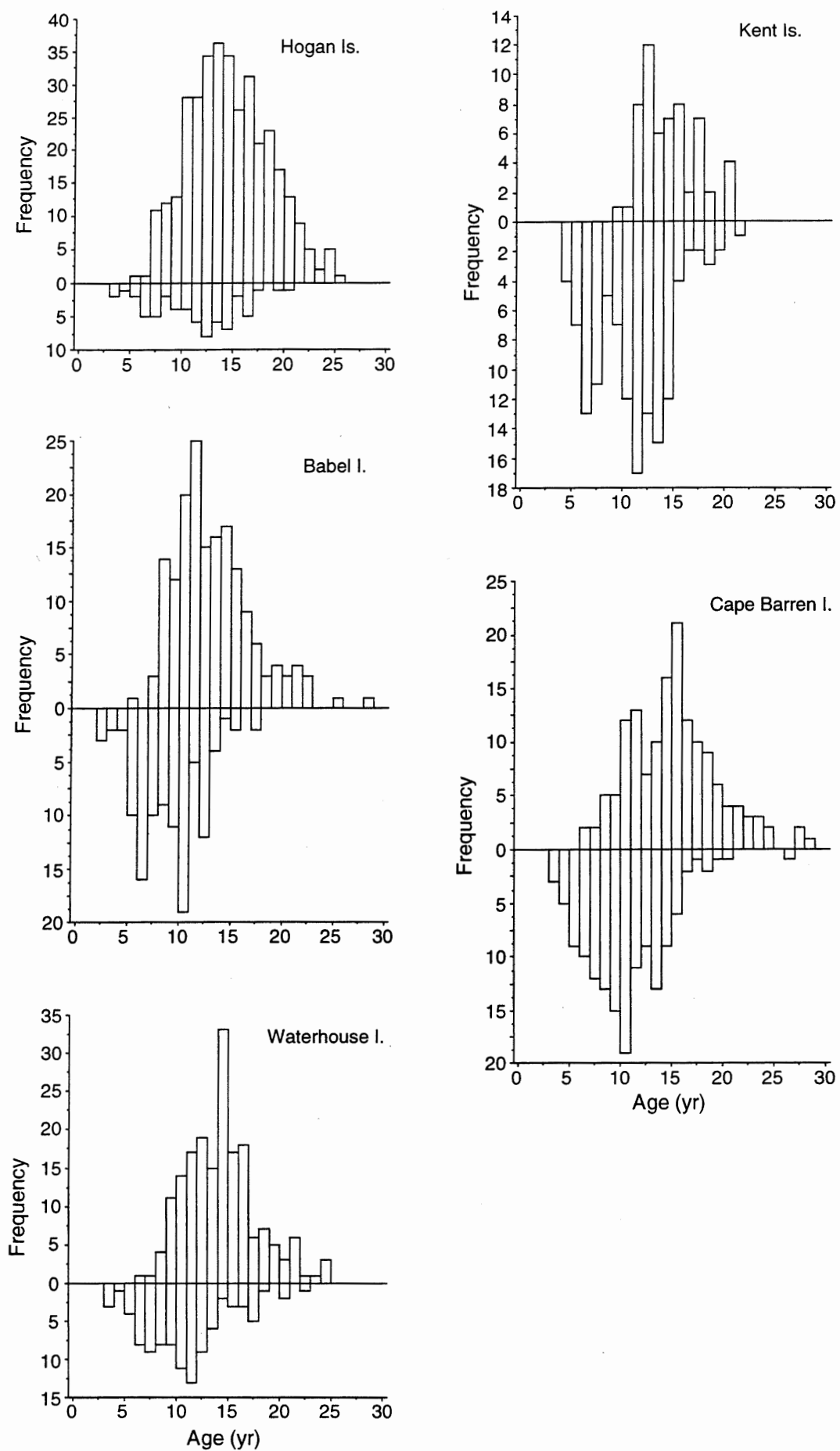


Figure 26. Age composition of cryptic and emergent blacklip abalone (*Haliotis rubra*) at each of the Bass Strait sites. Emergent abalone above the x-axis, cryptic abalone below the x-axis.

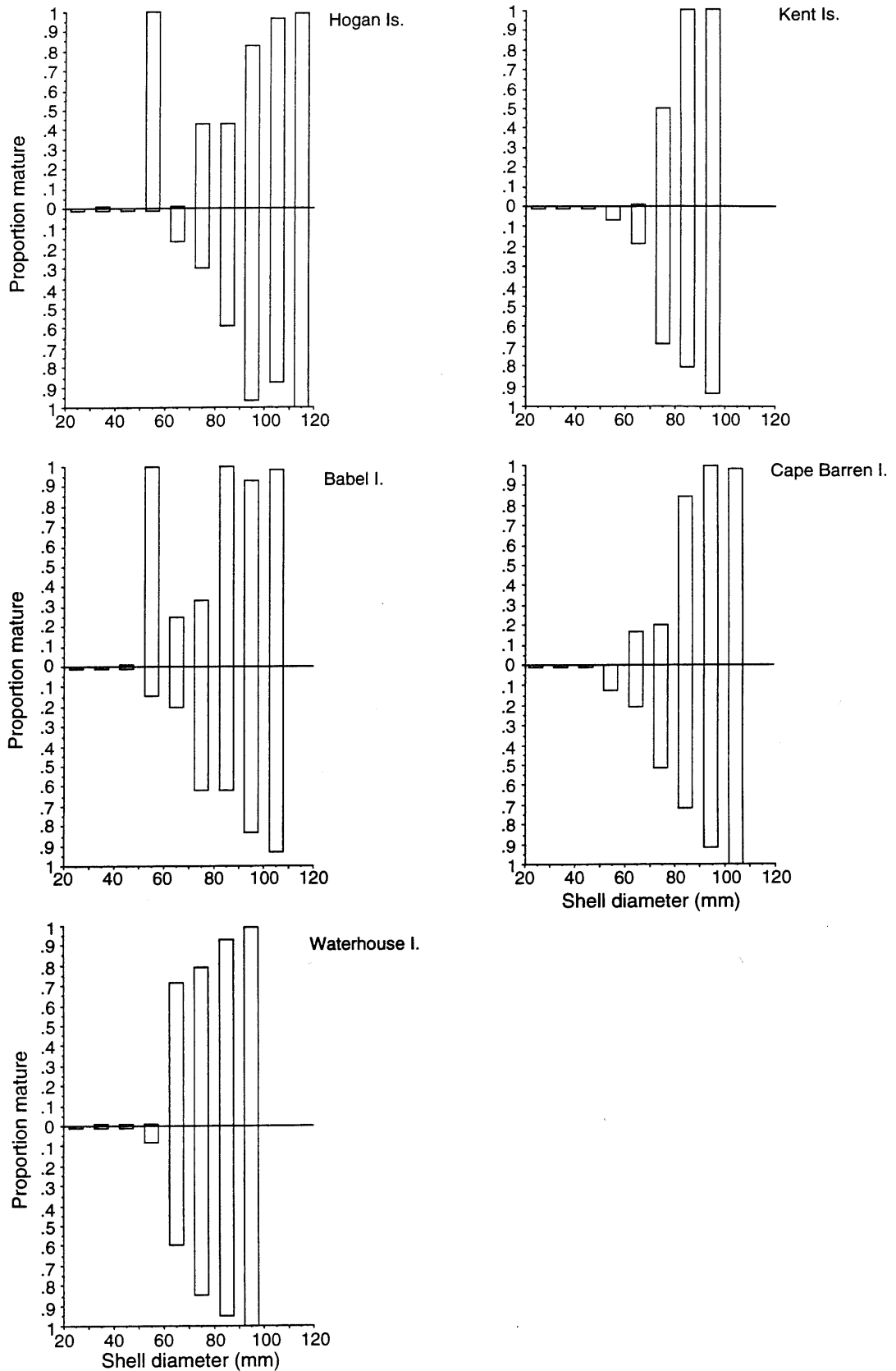


Figure 27. Relationship between shell diameter and sexual maturity for cryptic and emergent abalone at each of the five Bass Strait survey sites. Emergent abalone above the x-axis, cryptic abalone below the x-axis. Size classes for which the proportion mature was zero are shown as very short bars to distinguish them from size classes for which there were no animals.

Table 8. Instantaneous total mortality rates (Z), annual survival rates (S) and annual mortality rates (A) of *Haliotis rubra* at the five Bass Strait sites. Z was calculated both for 1 major growth ring per year and for 2 major growth rings per year (bold face). r^2 =coefficient of determination of the catch curve regression lines in Figure 15. n =no. of age classes used in the regression; $S = e^{-Z}$; $A = 1-S$. r^2 and n are the same for both regressions. See text for details.

Site	Z	r^2	n	S	A
Hogan Is.	0.219	0.899	14	0.803	0.197
	0.438			0.645	0.355
Kent Is.	0.250	0.959	12	0.779	0.221
	0.500			0.607	0.393
Babel I.	0.207	0.945	15	0.813	0.187
	0.414			0.661	0.339
C. Barren I.	0.185	0.933	17	0.831	0.169
	0.370			0.691	0.309
Waterhouse I.	0.265	0.892	11	0.767	0.233
	0.529			0.589	0.411

The occurrence of relatively low numbers of abalone in the early age classes (Fig. 15, bottom row) is due primarily to their cryptic behaviour. In the calculation of Z by catch curve analysis it is assumed that all age classes used (the modal age and older) are equally catchable. An examination of Fig. 25 suggests that this is not the case for the Kent and Cape Barren populations, where a substantial proportion of the animals used to calculate Z are cryptic; importantly, the proportion cryptic decreases markedly with size from the minimum length used to calculate Z . Cryptic abalone are, almost by definition, less catchable than emergent abalone because they are more difficult to see, so size-dependent variation in the proportion cryptic will cause the assumption of equal catchability to be violated. The effect of increasing catchability with size is to underestimate Z ; thus, the Z values derived here by catch curve analysis deserve to be viewed with caution, particularly in the Kent and Cape Barren populations. It is worth noting that the Cape Barren population has the lowest Z (Table 8).

In order to examine the effect that maturation-based catchability may have on the estimation of Z by catch curve analysis, Z was re-calculated for each of the five populations using only sexually mature animals. There was a resultant increase in Z for the Hogan, Kent and Cape Barren populations, a decrease for the Waterhouse population, and no change for the Babel Island population (Table 9). The greatest change in the Z estimate was 20 percent for the Hogan and Kent populations. This result supports the argument above that Z may be underestimated because of the cryptic fraction of the population in the age (or size) classes used to calculate Z . In all analyses requiring an estimate of Z (such as yield- and egg-per-recruit), the values obtained using all abalone, both mature and immature (Table 8), were used; the sensitivity of these per-recruit analyses to mortality rate variation is explored in Sections 3.6 and 3.7 below.

Table 9. Instantaneous natural mortality rates (Z) estimated by catch curve analysis for the five Bass Strait *Haliotis rubra* populations, using all animals (Z_1) and only sexually mature animals (Z_2). The difference between the two estimates is expressed relative to Z_1 .

Site	Z_1	Z_2	Difference (%)
Hogan Is.	0.219	0.262	19.6
Kent Is.	0.250	0.300	20.0
Babel J.	0.238	0.238	0.0
Cape Barron	0.185	0.190	2.7
Waterhouse I.	0.265	0.245	-7.5

When the proportion of sexually mature abalone that is cryptic was examined, it was found to decline with increasing size (Fig. 28). The effect of this would be to underestimate Z , as described above for all abalone (mature and immature).

A large proportion of the abalone sampled at each of the five sites could not be aged (Table 3, Fig. 12). If the ageable and non-ageable fractions of each population have dissimilar length compositions for those lengths which correspond to the age classes used to estimate Z , Z is likely to be inaccurate. Because this is clearly the case (Fig. 12), the age composition of the entire population sample, including unageable animals, was estimated using age-length keys: the relationship between age and length, derived from ageable animals (Fig. 16) was used to apportion unageable animals of a given size across the age classes. These estimated ages were then combined with the 'true' ages (measured by counting growth rings) to yield an age-frequency composition for the entire population sample. Z was then re-calculated by catch curve analysis and compared with the Z value obtained using only ageable abalone.

The Z estimates obtained using both ageable and unageable abalone combined was considerably higher than the Z values calculated using ageable abalone alone at all five sites (Table 10), with the increase ranging from 16.2 percent for the Waterhouse Island sample to 32.0 percent for the Hogan Islands sample. This result was contrary to expectations that arose from the ageable proportion, by size, of each population sample shown in Fig. 13. Fig. 13 shows that, for the Hogan sample, the proportion ageable declines with size, while the reverse applies to the Waterhouse Island sample. Catch curve analysis of the Hogan sample after inclusion of calculated ages of unageable abalone by age-length key analysis should therefore have increased the relative abundance of the older age classes, and the resulting regression line fitted to the log-transformed age-frequency data should have been less steep, and Z therefore less. The reverse argument would apply to the Waterhouse sample. A major reason for the increase in Z when the estimated ages of unageable abalone are included is that the modal age class was shifted to the

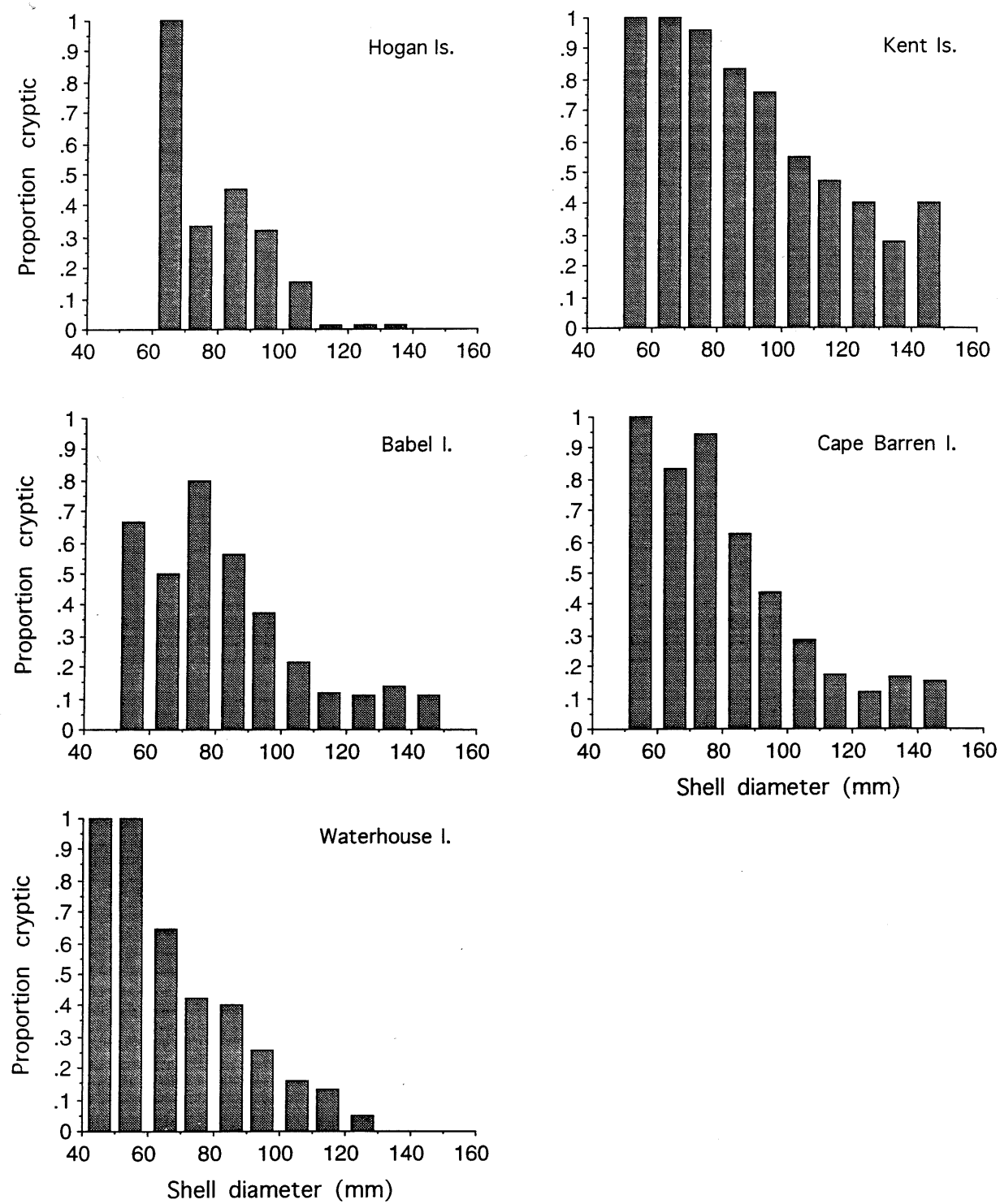


Figure 28. The relationship between size and the proportion of sexually mature blacklip abalone (*Haliotis rubra*) that are cryptic.

right by one or two years at all sites except Waterhouse Island. This is illustrated using the Kent Islands sample (Fig. 29).

These two factors (size-related crypsis and size-related ageability of abalone shells) both act to underestimate Z . The effect of the former was greatest for the Hogan and Kent populations, and the latter for the Hogan and Cape Barren populations; the Z estimate for the Hogan Islands is therefore likely to be the most severely underestimated.

Table 10. Instantaneous total mortality rates (Z) estimated by catch curve analysis of both ageable and non-ageable *Haliotis rubra* using age-length keys (Z_{tot}). Estimates of Z estimated using ageable abalone only (Z_{age}) are also shown for comparison. The estimates are based on a growth ring deposition rate of one per year. The difference between the two estimates is expressed relative to Z_{age} .

Site	Z_{tot}	Z_{age}	Difference (%)
Hogan Is.	0.289	0.219	32.0
Kent Is.	0.322	0.250	28.8
Babel I.	0.256	0.207	23.7
C. Barren I.	0.265	0.185	43.2
Waterhouse I.	0.308	0.265	16.2

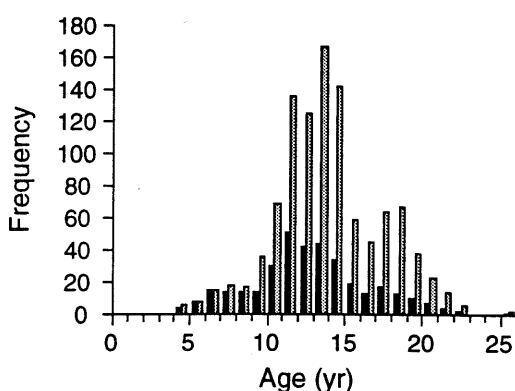


Figure 29. Age-frequency composition of *Haliotis rubra* from the Kent Islands plotted using only ageable individuals (■) and all individuals (▨), the latter estimate obtained using age-length keys.

3.6 Yield per recruit

The values of the various parameters required for the yield-per-recruit (YPR) analyses are given in Table 11. YPR relationships at the five sites are shown graphically in Fig. 30 (one growth ring per year) and Fig. 31 (two growth rings per year). The YPR values at various levels of F at sizes at first capture of 110 mm and 118 mm can be obtained from Figs. 30 and 31. The actual figures used to construct these isopleths are given in the Appendix (Table A.1). (The 110 mm size limit was in place for the 1989 Bass Strait fishing exercise, and 118 mm is the size at which an age class comprises 80-100 percent sexually mature individuals (Fig. 15), and also the minimum size limit during the 1991 Bass Strait stunted blacklip abalone fishing exercise.) At all sites, the size at which yield per recruit is maximal is substantially less than either 110 or 118 mm (Table 12A).

The sensitivity of the YPR analysis to the frequency of shell ring deposition was then examined. It was found that there were moderate differences between the results at low levels of F , with a decrease in this difference as F increased (Figs. 30, 31; Table A.1). The relative insensitivity of YPR to the number of growth rings per year may be attributed to the fact that the increase in Z is compensated for by the faster growth rate (and therefore higher productivity) that a two-rings-per-year relationship would cause (Table 11).

The sensitivity of YPR analysis to variation in M alone was then examined. If the Bass Strait *H. rubra* populations are subjected to fishing, then the estimates of Z calculated by catch curve analysis (Fig. 15; Table 8) are a combination of both natural and fishing mortality, and M is then less than Z . The YPR analyses were therefore repeated using two sets of M values, one 75 percent and the other 50 percent of Z . The sizes at which YPR is maximal at these two Z values for a range of F values are shown in Tables 12B and 12C. When these values are compared with those under the no-fishing scenario (Figs. 30, 31), yield per recruit is invariably higher. (This is always the case: the lower the value of M , the longer the animal should be left before harvesting because biomass attrition overtakes biomass increase at a later age.) Increase of YPR as M decreases is particularly pronounced at low levels of F . At a minimum size limit of 110 mm at Hogan Islands, for example, YPR at a fishing mortality of 0.2 (annual mortality of c. 19 percent) is 48.6 percent of B_{max} when $M=Z$, 64.6 percent if $M=0.75*Z$ and 81.0 percent if $M=0.5*Z$. These detailed YPR values are given in Tables A.1 ($M=Z$), A.2A ($M=0.75*Z$) and A.2B ($M=0.5*Z$) in the Appendix. The sensitivity of YPR to variation in M is clearly demonstrated.

Table 11. Values of the parameters used in the calculation of yield per recruit and egg per recruit for *Haliotis rubra* at the five Bass Strait survey sites. Parameter estimates were derived for both 1 and 2 shell growth rings per year. L_∞ , K and t_0 : von Bertalanffy growth parameters; M : instantaneous rate of natural mortality; t_λ : maximum age; a , b : parameters of the logistic maturation-by-length equation (Equation 2); c , d : parameters of the length-whole weight equation (Equation 1); p , q : parameters of the length-fecundity equation (Equation 3).

Site	1 growth ring/yr				2 growth rings/yr				t_λ	a	b	c	d	p	q
	L_∞	K	t_0	M	L_∞	K	t_0	M							
Hogan Is.	135.7	0.168	3.508	0.219	135.7	0.336	1.754	0.438	25	-12.77	0.155	0.0001495	2.962	0.0000116	3.196
Kent Is.	127.0	0.135	2.388	0.250	127.0	0.270	1.194	0.500	25	-8.073	0.110	0.0000831	3.087	0.0000163	3.207
Babel I.	146.1	0.136	2.863	0.207	146.1	0.272	1.432	0.414	25	-8.517	0.123	0.0001083	3.040	0.0000523	3.004
C. Barren I.	139.4	0.129	2.634	0.185	139.4	0.258	1.317	0.370	25	-10.96	0.145	0.0000773	3.122	0.0000750	2.894
Waterhouse I.	121.6	0.151	2.545	0.265	121.6	0.302	1.273	0.530	25	-11.12	0.170	0.0000888	3.095	0.0000385	3.186

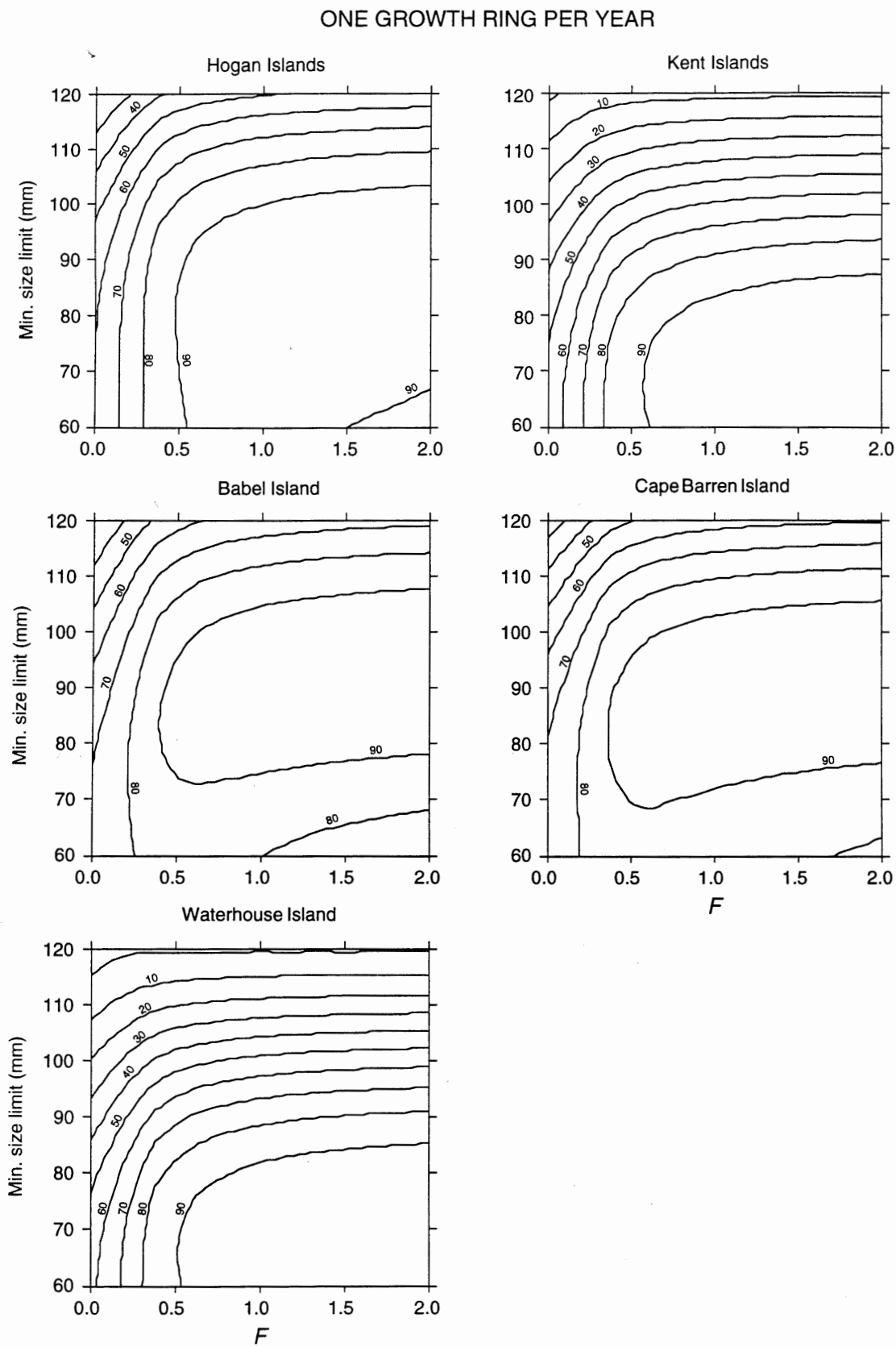


Figure 30. Yield-per-recruit contour diagram for *Haliotis rubra* from the five Bass Strait sites, analysed with growth and natural mortality parameter values calculated from one shell growth ring per year.

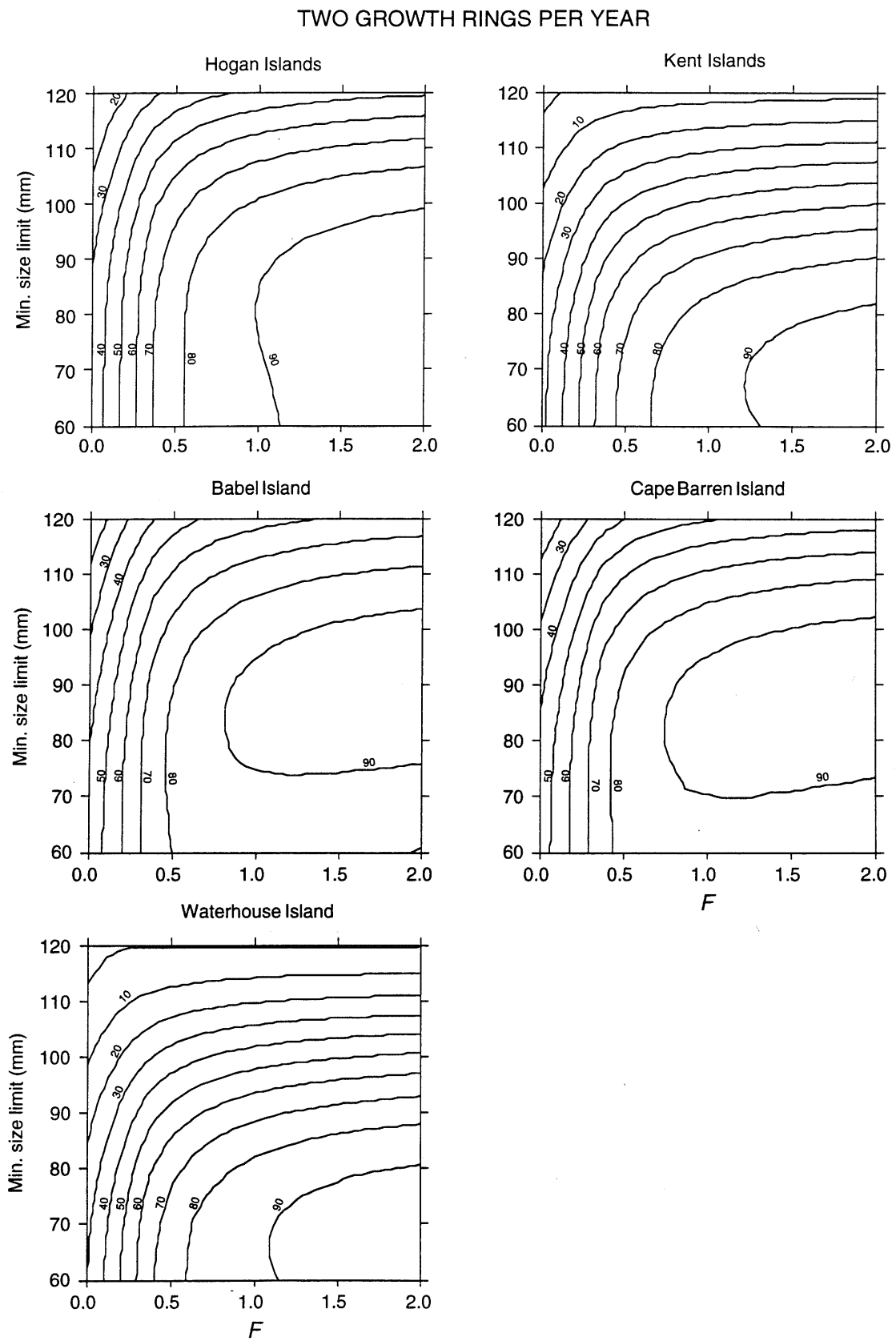


Figure 31. Yield-per-recruit contour diagram for *Haliotis rubra* from the five Bass Strait sites, analysed with growth and natural mortality parameter values calculated from two shell growth rings per year.

Table 12. Size (maximum shell diameter, in mm) at which yield per recruit is maximal at a range of fishing mortality (F) values for *Haliotis rubra* at each of the five Bass Strait sites, when (A) $M=Z$; (B) $M=0.75*Z$; and (C) $M=0.5*Z$.

(A)

Site	No. growth rings	<i>F</i>				
		0.4	0.8	1.2	1.6	2.0
Hogan Is.	1	79.9	85.3	88.5	90.1	91.6
	2	74.0	79.9	83.5	85.3	88.5
Kent Is.	1	65.8	70.6	73.6	75.0	75.0
	2	58.9	64.2	69.1	70.6	72.1
Babel I.	1	83.5	90.0	93.0	94.4	94.4
	2	75.4	84.4	89.2	90.7	90.7
Cape Barren I.	1	84.1	89.5	90.8	92.0	93.2
	2	76.5	84.1	88.2	89.5	90.8
Waterhouse I.	1	64.9	69.8	72.9	74.3	74.3
	2	59.5	64.9	68.2	71.4	71.4

(B)

Site	No. growth rings	<i>F</i>				
		0.4	0.8	1.2	1.6	2.0
Hogan Is.	1	91.6	95.8	97.2	99.7	99.7
	2	83.5	90.1	93.1	95.8	97.2
Kent Is.	1	76.4	81.6	83.9	85.1	85.1
	2	69.1	76.4	80.3	80.3	81.6
Babel I.	1	94.4	101.0	102.2	103.4	104.5
	2	87.6	95.1	99.1	100.3	101.6
Cape Barren I.	1	94.4	98.8	99.9	100.9	102.3
	2	86.9	94.9	97.8	98.8	99.9
Waterhouse I.	1	74.3	79.7	82.2	82.2	83.3
	2	68.2	75.7	77.1	79.7	80.9

(C)

Site	No. growth rings	<i>F</i>				
		0.4	0.8	1.2	1.6	2.0
Hogan Is.	1	102.0	98.0	107.7	109.1	109.1
	2	94.5	102.0	105.2	106.2	98.0
Kent Is.	1	90.4	93.2	94.6	95.9	95.9
	2	82.8	89.4	92.3	92.3	94.1
Babel I.	1	108.8	112.6	114.0	115.3	115.3
	2	101.6	109.3	111.2	113.1	98.3
Cape Barren I.	1	106.4	110.0	111.1	111.1	112.2
	2	100.9	106.4	108.0	109.6	109.6
Waterhouse I.	1	86.6	90.1	91.5	92.9	92.9
	2	80.9	86.6	88.7	90.6	90.6

3.7 Egg per recruit

The values of the various parameters required for the egg-per-recruit (EPR) analyses are shown in Table 11. EPR relationships at the five sites are shown graphically in Fig. 32 (one growth ring per year) and Fig. 33 (two growth rings per year). The actual figures used to construct these EPR isopleths are given in the Appendix (Table A.3).

When the sensitivity of the EPR analysis to the frequency of shell ring deposition was examined, it was found that there was little difference between the results when size at first capture was $\geq c.$ 100 mm (Figs. 32, 33; Table A.3). As with YPR, this may be attributed to the fact that the increase in Z is compensated for by the faster growth rate (and therefore higher productivity) that a two-rings-per-year relationship would cause (Table 11).

The sensitivity of EPR analysis to variation in M alone was then examined using the same estimates of M as in the YPR results above (75 and 50 percent of Z). When these results are compared with those under the no-fishing scenario, EPR decreases as M decreases. At a minimum size limit of 110 mm at Hogan Islands, for example, population egg production at a fishing mortality of 0.2 is 70.6 percent of the egg production of the unfished population when $M=Z$, 62.0 percent if $M=0.75*Z$ and 52.1 percent if $M=0.5*Z$. These detailed EPR values are given in Tables A.3 ($M=Z$), A.4A ($M=0.75*Z$) and A.4B ($M=0.5*Z$) in the Appendix. Derivation of these various EPR results using a range of possible parameter values allows an assessment of the impact of fishing on these abalone stocks to be made at several degrees of conservatism. Further assessment of the sustainability of fishing levels by population modelling (with the incorporation of spawning stock biomass-recruitment relationships)—not considered further here—can be made using these various parameter estimates.

4 DISCUSSION

4.1 Morphometrics

Morphometric analyses were carried out in order to quantify the variability between sites, as well as to allow the detection of any changes in length-weight-shape characteristics that may occur through time. The second of these reasons is particularly relevant to populations that presently are relatively unfished; at present, this applies almost solely to the slow-growing stunted populations. There is anecdotal evidence provided by divers that, at least in some areas, shell quality improves and growth rates increase as a population of abalone is fished; density-dependent growth rates are implied. It is important for the future management of these abalone stocks to document this.

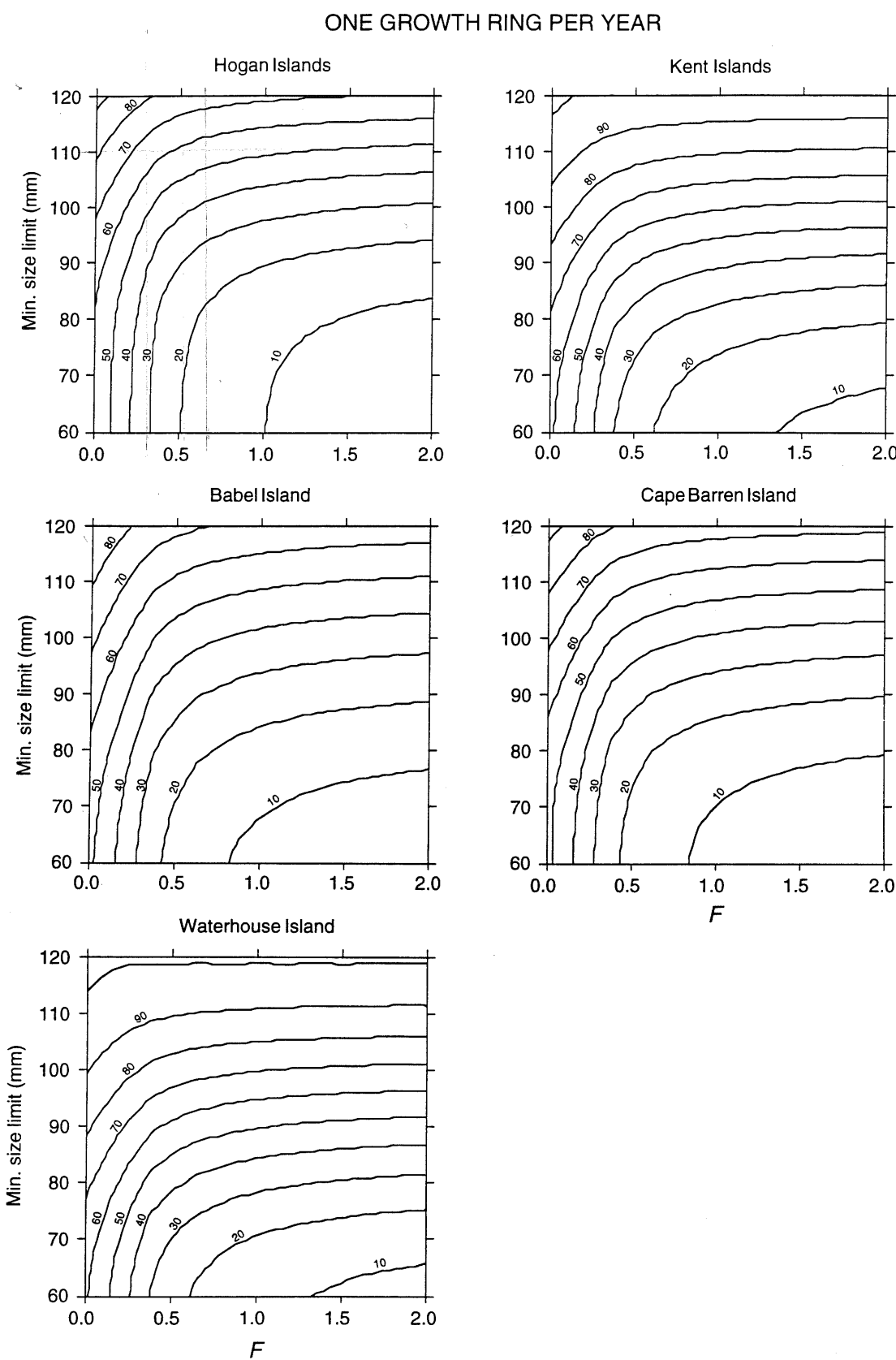


Figure 32. Egg-per-recruit contour diagram for *Haliotis rubra* from the five Bass Strait sites, analysed with growth and natural mortality parameter values calculated from one shell growth ring per year.

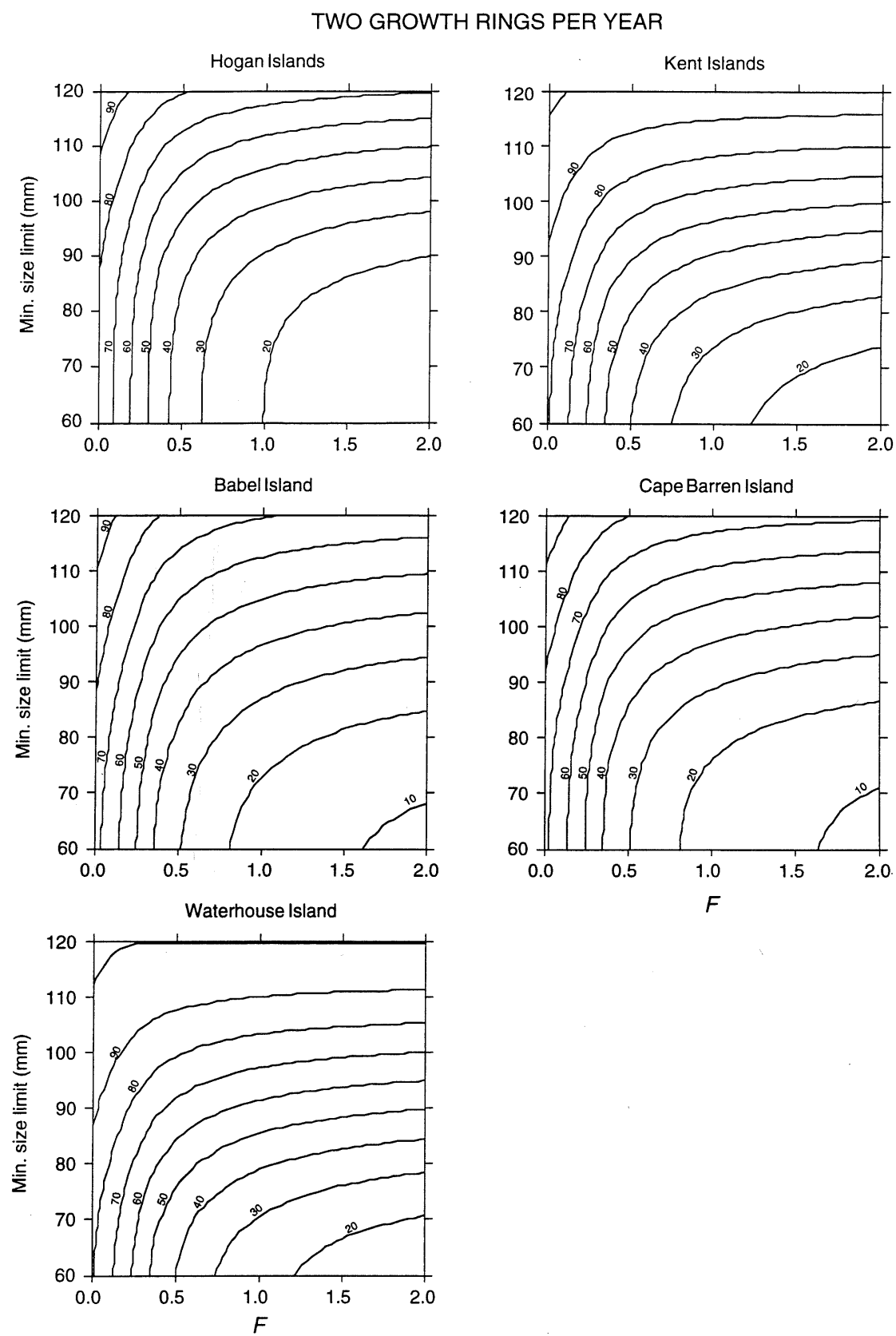


Figure 33. Egg-per-recruit contour diagram for *Haliotis rubra* from the five Bass Strait sites, analysed with growth and natural mortality parameter values calculated from two shell growth rings per year.

4.2 Growth and ageing

The cause(s) of growth checks in the shell of abalone have been determined or postulated for some abalone. For example, an annual mark was formed at the time of gonad maturation and spawning in *Haliotis discus hannai* (Sakai 1960) and *H. d. discus* (Kojima 1975), while a seasonal (temperature) effect was reported in *H. australis* (Poore 1972) and *H. diversicolor aquatilis* (Kim and Chung (1985). It is now argued that the observed pattern of larger mean size of mature than immature abalone within an age class (Fig. 19) provides circumstantial evidence that the growth checks in the spire of *Haliotis rubra* are not related to reproduction. (Note that checks related to reproduction, such as those just cited, have been shown only for the growing edge layers, not the spire of the shell.) If shell growth checks are formed in relation to reproduction as well as to seasonal (presumably temperature-related) factors, this would affect the apparent age (measured as the number of shell rings): abalone of a given age which had reached sexual maturity, and which had spawned, would have more shell rings than abalone of the same age which had not spawned. The spawners would therefore be wrongfully assigned to an older age class. A putative age class would then include abalone which had spawned whose true age was less than that of the immature members of the age class. The effect of this would be to underestimate the size at age of mature abalone, which, in turn, would tend to obliterate the observed pattern shown in Fig. 19 (mature abalone being consistently larger than immature abalone of the same apparent age). The notion that shell rings in the spire are deposited, at least in part, in relation to spawning, therefore is not supported. This conclusion supports that of de Jong (1990) who, in a detailed analysis of shell layer deposition in *Haliotis rubra*, presented evidence that layers deposited under the spire of the shell are related only to seasonal factors, whereas the layers at the growing margin of the shell are related to both season and reproduction.

The proportion of a population sample that could be aged in this study (33 to 46 percent) was similar to the ageable fraction at two sites in Victoria (31 and 46 percent) (McShane and Smith 1992); none of the abalone at a third site in Victoria could be aged. McShane and Smith concluded that growth checks are of little use for ageing *H. rubra* because of variable frequency of shell checks and the probable bias in the age-length relationship caused by the low proportion of shells that could be aged. Ageing by shell growth checks of *H. rubra* from approximately 30 sites around Tasmania has shown that the proportion of ageable shells in the Bass Strait populations is the exception rather than the rule; elsewhere it ranges from 60 to more than 90 percent (unpublished results). In addition, marginal increment analysis has shown that shell layers are deposited once per year (*i.e.*, one aragonite and one conchiolin layer per year) (Nash *et al.* in prep. *a*). Furthermore, the distinction in size between immature and mature abalone within a putative age class (Fig. 19) is evidence that the relationship between number of

growth rings and age is close. McShane and Smith's conclusion that ageing of *H. rubra* by growth checks is generally of little use therefore seems premature.

Since many of the analyses and conclusions presented here depend on the relationship between numbers of shell layers and age, it is important that ageing verification studies be conducted throughout Tasmania. As discussed below, however, the yield- and egg-per-recruit results are not greatly affected by the number of shell growth rings per year.

4.3 Sexual maturation and fecundity

4.3.1 Onset of sexual maturity

This study has shown that sexual maturation commences at about six years of age (assuming one growth ring per year), and a steadily increasing proportion of successively older year classes is mature. Nearly all (80 to 90 percent) of the animals in a year class are mature at 10 to 12 years of age.

The graphs in Fig. 15 show that full recruitment at all five sites (and at all other sites so far surveyed around Tasmania: unpublished data), occurs approximately at the age at which all animals of that age are sexually mature. From this it is inferred that abalone emerge from the sub-boulder habitat at onset of sexual maturity; all subsequent age/size classes are therefore of equal catchability. Thus, the maturation ogive for each site functions, in effect, as a fishing selectivity ogive. It was therefore incorporated as such into the yield- and egg-per-recruit analyses above.

When the emergence-at-maturity hypothesis was examined directly, however, it was not clearly supported (Fig. 27). This hypothesis is important from the point of view of increasing catchability with size as sexual maturity is reached because of its effect on the calculation of instantaneous total mortality (Z) by catch curve analysis. Yet even among the sexually mature fraction of each of these populations the degree of crypsis declined with size (Fig. 28). The ability to be cryptic depends to a large extent on the complexity of the substrate: complex bottom (big boulders and/or lots of crevices) afford shelter for abalone of all sizes, whereas opportunity to hide will decrease sharply with increasing abalone size when the substrate is simple. Substrate complexity will determine the ability of an abalone to hide, regardless of its sexual condition; when few crevices are available, or if these are small, abalone will be forced into the open as they grow, regardless of sexual condition. It is therefore clear that the validity of the emergence-at-maturity hypothesis is closely related to substrate type and complexity. Although the emergence-at-maturity hypothesis is not clearly supported by the direct evidence

(Fig. 27), it is difficult to find an alternative explanation for the observation (Fig. 15) that the modal age class is consistently very close to the first fully mature age class.

The distinction between cryptic and emergent abalone is not always clear. The question of how hidden an abalone had to be to be defined as cryptic was difficult to answer during the survey. Different research divers used their own interpretations of cryptic and emergent. The criterion finally used in this and subsequent surveys was that, if an abalone could be seen at all without turning boulders or otherwise disturbing the substrate, it was emergent; if an abalone could be felt but not seen it was cryptic. All other abalone were cryptic.

The proportion of cryptic abalone in a population sample depends on substrate type: in general (and by our definition of cryptic), cryptic abalone are scarce in open terrain, whereas in complex boulder bottom they are more abundant. Complex bottom may be further divided into boulders that can be turned and those that are too large to move. Highest numbers of cryptic abalone are to be found under the former (unless the boulders are embedded in sand, in which case there are no cavities for the abalone to live in). It therefore seems unlikely that a completely satisfactory practical definition of ‘cryptic’ can be found.

Any conclusions drawn about the level of egg production conserved under a given size limit/fishing mortality regime depend on the validity of the inference that abalone become catchable at the onset of sexual maturity. The sensitivity of the EPR analyses to this conclusion was therefore examined by repeating the EPR analyses with selectivity not incorporated. It was found that, at all sites, the effect was negligible at size limits greater than c. 90 mm (results not shown); this is attributable to the fact that maturation by this size is almost complete (Fig. 20). Thus, these analyses are not sensitive to the hypothesis that *Haliotis rubra* emerges at onset of sexual maturity.

4.3.2 Fecundity

As an index of fecundity, gonad volume represents the potential fecundity only; this will be less than the true fecundity unless all eggs in the gonad are released at spawning, which Clavier (1992) found was not so for *H. tuberculata*. If the proportion of ripe gametes that are released at spawning is not size-dependent, the results of the EPR analyses will not be affected. However, it is not clear that the use of potential fecundity will yield the same age-relative fecundity relationship as the use of the realised fecundity, because experience in abalone hatcheries suggests that younger, smaller abalone are more vigorous spawners, and spawn more frequently, than larger, older abalone (T. Lewis, K. Hahn, pers. comms.). If this is true for wild abalone as well, the relationship between age and fecundity would be ‘flatter’ (less

steep) than the volumetric index of fecundity, used here, would suggest. The effects of this flattening on the EPR analyses would be to reduce the sensitivity of the relationship between minimum legal size and egg per recruit; in other words, a higher size limit would not afford the increase in protection of egg production that the results presented here (Figs. 32 and 33, Tables 15 and 16) would indicate.

The use of gonad volume as a measure of fecundity also assumes that the length-gonad volume relationship or the age-gonad volume relationship does not, in relative terms, vary greatly throughout the gametogenic cycle. This assumption needs to be tested because it is not always possible to sample a population when it is in peak reproductive condition. This may not be as critical for *H. rubra* as other abalone species because the spawning period of this species in Tasmania is protracted (unpublished data).

The scatter of points on both the age-fecundity and length-fecundity plots (Figs. 21, 22) is very wide. In the absence of direct fecundity measurements (number of ripe ova in the gonad) it is not possible to determine how much this is because of true variation in fecundity and how much is caused by measurement error. Reproductive studies of *H. rubra* in southern Tasmania have shown that there may be considerable variation in reproductive condition (and therefore fecundity) between individuals sampled at the same time (unpublished data); moreover, the extended spawning period of this species will produce a wider fecundity range than in species with closely synchronous spawning. Measurement error may be caused by either an imprecise relationship between true fecundity and cross-sectional gonad area (the measure of fecundity used here) or inaccurate tracing of the gonad cross-sectional area. Error caused by the former is probably not major, since the relationship between gonad cross-sectional area and gonad volume is reasonably close ($r^2=0.78$: Fig. 9). Error in tracing the gonad is affected by the pressure applied to the conical appendage section against the tracing surface. Although light pressure was applied to all sections, some variation would have been unavoidable. In addition, the conical sections were traced when frozen or slightly thawed, so the variation in tissue hardness would have been a source of error in traced area.

In order to examine the effect that variable pressure would have on the cross-sectional gonad area, 12 sections (four female and eight male) were measured at normal (slight) pressure and again at high pressure. Gonad area was 23 percent larger (± 14.5 percent standard deviation) at high pressure, relative to the gonad area at light pressure, for females; the corresponding values for males was 42 percent (± 26 percent). The high pressure applied was deliberately higher than that applied routinely in this study, but this comparison does indicate that variable pressure applied when tracing the conical appendage section may be a significant component of the error associated with the measurement of fecundity. In future studies of this sort, it will therefore be

important that the conical appendage be hardened in a fixative (ethanol, for example) prior to measuring its cross-sectional area.

The residuals analysis of the age-length-fecundity relationships (Fig. 24) show that fecundity is primarily a function of size. From this it may be inferred that rapid growth in size (*i.e.* somatic growth) does not take place at the expense of reproductive development; when conditions are good for growth, growth of both somatic and reproductive tissues benefits (Fig. 24B). The interesting implications of these results in the light of resource allocation theory (*e.g.*, Kozlowski 1992; Taylor and Gabriel 1992) will not be explored further here.

4.4 Mortality

The accuracy of the determination of instantaneous total mortality from the slope of the descending limb of the log-transformed age frequency distributions (Fig. 15, bottom row) relies on several assumptions: (i) that these age classes are equally vulnerable to sampling; (ii) that recruitment rates to the populations are constant through time; (iii) that mortality rates do not change with age in the fully recruited year classes; and (iv) that the mortality rate is constant over time. Because some of the age classes used in the estimation of Z included immature animals, and because the evidence of Fig. 15 suggests that immature animals are less vulnerable to capture (*i.e.*, are more cryptic) than mature animals, assumption (i) would appear to be violated. When determining the population age structure using growth rings, as was done here, a further assumption is that ageability is not age-dependent. It was not expected that the proportion of ageable shells would increase with size, as occurred in the Kent, Babel and Waterhouse populations; the opposite was expected because shell quality is likely to deteriorate with age. One possible explanation is that the largest abalone are not the oldest abalone. This could occur if growth and survival rates were inversely related (fast-growing animals do not live to old age, and *vice versa*). Evidence to support this is meagre: the age-length scatterplots sometimes tend to show a dome-shaped distribution rather than an asymptotic one (Figs. 15M, 16, and unpublished data from other sites). It therefore seems unlikely that this effect is strong enough to cause the proportion of non-ageable shells to be highest at small shell size.

The assumption of constant mortality across the fully recruited age classes has not been examined in northern Tasmanian abalone populations; however, Prince *et al.* (1988b) have shown that mortality rates in a southern Tasmanian *Haliotis rubra* population (at George III Reef) were nearly constant in all but the youngest age classes (0 to 3.5 years). Mortality estimation in the present study commenced with the 11 to 15 year age class (Fig. 15, bottom row), well above the age at which the mortality for *H. rubra* at George III Reef had become virtually constant.

If there were a marked decrease in mortality with increasing age at the five survey sites described here, it would be evident as a trend in the frequency of the fully recruited age classes; these would form a curve that was concave upward. It can be seen (Fig. 15, bottom row) that this is not the case at any of the sites. The available evidence therefore suggests that the assumption of constant mortality rates for the fully recruited age classes has not been violated.

Although it is probable that recruitment rates are not strictly constant (assumption (ii) above), it is reasonable to assume that, on average, they have been in the five areas surveyed. This is because the regression lines fitted to the fully recruited age classes in Fig. 15 (bottom row) are, in effect, the average slope across 9 to 14 age classes. Bias in Z because of trends in fishing is unlikely to be major because these sites have been protected to a large degree from heavy fishing by their slow growth and low maximum sizes. Any fluctuations in recruitment rates are therefore likely to have been random natural ones.

Fluctuations in recruitment rate between years would be reflected in an increased scatter of points about the regression lines fitted to the descending limb of the catch curves (Fig. 15, bottom row). If recruitment rates were undergoing a steady directional change (as might happen in response to a decline in the reproductive stock, caused by fishing), the resulting catch curve would still be linear but have a lower slope. Because these Bass Strait stocks have been protected from fishing by their small sizes, relative to the minimum legal size limit (as argued above), it is unlikely that fishing-induced changes in recruitment rates have occurred. Hence, recruitment rate variation is not likely to have affected the estimation of Z by catch curve analysis.

Evidence to support this comes from recent studies of settlement rates of *H. rubra* larvae, which show that spawning and settlement extend over several months of the year (unpublished results). If it is assumed that environmental factors which may affect rates of settlement and post-settlement survival are time-independent (*i.e.*, equally likely to occur at all times of the year and at any frequency) then, although within-year variation in recruitment rate may be fairly large, between-year variation will likely be small. In other words, the range of survival rates of recruits that may be experienced will likely occur within the space of a single year; it is less likely that the overall rate of recruitment (averaged out over an entire year) will vary greatly between years. In this respect, it is reasonable to expect that inter-annual variation in recruitment rate would be far higher for a species (such as scleractinian corals: Babcock *et al.* 1986) which spawns on only one day of the year; for such species, the chance of recruitment failure for the entire year due to adverse environmental conditions is likely to be much greater. Thus, inter-annual variation in *H. rubra* recruitment rates is likely to be small.

Estimation of Z using age-length keys assumes that the age-length relationship (*i.e.*, growth rate) of unageable and ageable abalone is the same. If, within a site, shell condition deteriorates with age then non-ageable shells are likely to be older than ageable shells of the same size. This effect is, in turn, likely to be affected by other factors such as the microhabitat in which an abalone lives: those living on exposed upper rock surfaces appear to be less prone to infestation by boring worms and sponges than those living in more sheltered places (unpublished observations). It is difficult to see how violation of this assumption would affect the estimation of Z; it may cause a lateral (*x*-shift) of the regression line, or it may affect the slope of the line itself.

An important effect of the Z values derived using age-length keys is that, in four of the five populations, the modal age is shifted to the right of the age at full maturity shown in Fig. 15 (Fig. 29). The effect of this on the emergence-at-maturity hypothesis cannot be assessed because the maturation curves (Fig. 15, middle row) are no longer strictly comparable; and the maturation data cannot be augmented with the data for the unageable abalone because it is impossible to assign age to individual abalone for which there is maturity information.

It is important to note that the problems and complexities of parameter estimation caused by the existence of unageable abalone do not exist, or are negligible, for almost all other sites in Tasmania where population samples have been taken, because the unageable proportion of shells is very small (unpublished results).

The extent of fishing for *H. rubra* in the areas sampled during this survey are not known, but the following information was provided in late 1988 by commercial abalone divers, rock lobster fishermen and the lighthouse keeper on Deal Island (in the Kent group) concerning rates of fishing in the five areas visited. The Kent Islands are reportedly fished regularly by Victorian divers. The Hogan Islands are fished less by the Victorians, despite their closer proximity to Victoria, largely because the anchorages are not as good as at Kent. Babel and Cape Barren Islands are fished by divers in the Furneaux group, but the amount is not large because only a small proportion of the abalone taken by the Furneaux divers is blacklip abalone; more than 80 percent of the catch is greenlip abalone (*H. laevigata*). Divers have reported, however, that the undeclared catch of blacklip abalone from Babel Island has been substantial. The Waterhouse Island area is not fished apart from light amateur fishing pressure. These reported fishing patterns are not closely correlated with the estimated total mortality rates (Table 8), suggesting that rates of natural mortality vary between the sites.

4.5 Yield per recruit and egg per recruit

This study has yielded estimates of population parameters that are necessary for yield- and egg-per-recruit analyses. Future assessments of these stunted populations may now be made using estimates of fishing mortality derived during short-term fishing exercises on these populations during 1989 and 1991 (Nash *et al.* in prep. b).

If there were no relationship between stock size and subsequent recruitment, the abalone stocks could be managed to maximise the yield from a cohort by lowering the size limit to less than 100 mm at all sites (if the stocks at the time of sampling were essentially unfished). If the stocks were fished at the levels considered above (one-quarter and one-half of Z), a reasonably high proportion of the yield per recruit is taken by fishing at moderate to high levels of fishing pressure (Table 14). However, because evidence from other abalone populations (British Columbia: Breen, 1986; Mexico: Guzmán del Próo 1989; California: Tegner *et al.* 1989) indicates that abalone fisheries are prone to collapse because of recruitment failure (although whether this is directly caused by recruitment overfishing has not been established: Breen 1992), it is necessary to consider the proportion of egg production that is protected at various size limit. This is accomplished using egg-per-recruit analysis.

Perhaps the most important result to arise from these analyses is that egg per recruit is relatively insensitive to the rate of shell layer deposition (Figs. 32, 33; Tables A.3, A.4). The reason for this is apparently related to the interrelationship between Z and growth rates: as the number of layers deposited per year increases, Z (derived by catch curve analysis) increases, and so does growth rate (Table 11). When M alone is varied, variation in EPR is considerably greater (Tables A.3, A.4). The rate of shell layer deposition is therefore not crucially important for stock assessment by EPR analysis, although its importance for other reasons, such as determining the time lag between spawning and recruitment to the fishery, is not diminished.

5 ACKNOWLEDGEMENTS

This research was funded by the Sea Fisheries Division, Tasmanian Department of Primary Industry and Fisheries. Many thanks to Tony Wurf for making his vessel *Kobus* available for this survey, and to the Tasmanian Abalone Divers Research and Development Trust (TADRADT) for its role in organising the survey. Thanks also to the divers, deckhands, cook and other assistants for their assistance at sea: Jack Bock, Nigel Wallace, Wayne Blacklow, Paul Richardson, Peter Poulson, Gene Clifford, Kim Burgess-Watson, Craig Sanderson, and Jim and Louise Standish. The following people assisted with abalone processing and data entry: James Bridley, Martine Lamaury-Nash, Melissa Millington, Chris Lohberger, Roger

Kirkwood and Natalie Wickham. I am grateful to Keith Sainsbury, Scoresby Shepherd, Rob Day and Tony Harrison for helpful discussions, and to Rob Day and Scoresby Shepherd for critically reviewing an earlier version of this report. Bob Kennedy provided valuable assistance with computer programming.

6 REFERENCES

- Babcock, R.C., G.D. Bull, P.L. Harrison, A.J. Heyward, J.K. Oliver, C.C. Wallace and B.L. Willis 1986. Synchronous spawnings of 105 scleractinian coral species on the Great Barrier Reef. *Marine Biology* 90: 379-394.
- Breen, P.A. 1986. Management of the British Columbia fishery for northern abalone (*Haliotis kamtschatkana*). In G.S. Jamieson and N. Bourne (ed.): *North Pacific Workshop on Stock Assessment and Management of Invertebrates*. pp. 300-312. Canadian Special Publication in Fishery and Aquatic Sciences 92.
- Breen, P.A. 1992. A review of models used for stock assessment in abalone fisheries. In S.A. Shepherd, M. Tegner and S.A. Guzmán del Próo (eds.): *Abalone of the World: biology, fisheries and culture*. pp. 253-275. Blackwell: London.
- Clavier, J. 1992. Fecundity and optimal sperm density for fertilization in the ormer (*Haliotis tuberculata* L.). In S.A. Shepherd, M. Tegner and S.A. Guzmán del Próo (eds.): *Abalone of the World: biology, fisheries and culture*. pp. 86-92. Blackwell: London.
- Clavier, J. and O. Richard 1985. Études sur les ormeaux dans la région de Saint-Malo. *Association pour la mise en valeur du littoral de la Côte d'Emeraude*. 285 pp.
- de Jong, J. 1990. The relationship between age and growth of the blacklip abalone, *Haliotis rubra* (Leach) in Port Phillip Bay, Victoria. *Honours thesis, University of Melbourne*.
- Guzmán del Próo, S. 1989. Problemas y perspectivas de las investigaciones pesqueras sobre los abulones de México. *Proceedings of the Workshop Australia-México on Marine Sciences*, ed. E.A. Chavez. pp. 297-310.
- Hilborn, R. and C.J. Walters 1987. A general model for simulation of stock and fleet dynamics in spatially heterogeneous fisheries. *Canadian Journal of Fishery and Aquatic Sciences* 44: 1366-1369.
- Kim, J.-W. and S.-C. Chung 1985. On the growth of abalone, *Sulculus diversicolor diversicolor* (Reeve) and *S. diversicolor aquatilis* (Reeve), in Cheju Island. [In Chinese.] *Bulletin of the Marine Research Institute of Cheju National University* 9: 39-50.
- Kojima, H. 1975. A study on the growth of the shell of *Haliotis discus discus* (Gastropoda: Haliotidae) – I. Age and growth. [In Japanese.] *Aquaculture* 23: 61-66.
- Kozlowski, J. 1992. Optimal allocation of resources to growth and reproduction: implications for age and size at maturity. *Trends in Ecology and Evolution* 7: 15-19.
- McShane, P.E. and M.G. Smith 1992. Shell growth checks are unreliable indicators of age of the abalone *Haliotis rubra* (Mollusca : Gastropoda). *Australian Journal of Marine and Freshwater Research* 43: 1215-1219.
- Muñoz-Lopez, T. 1976. Resultados preliminares de un método para determinar edad en abulones (*Haliotis* spp.) de Baja California. [Preliminary results of a method for determining the age of abalone (*Haliotis* spp.) of Baja California.] *Memorias del Primer Simposium Nacional de Recursos Pesq. Masivos. Special volume on abalone and lobster. S.I.C. Inst. Nal. Pesca, México*. pp. 281-300.
- Nash, W.J. 1992. An evaluation of egg-per-recruit analysis as a means of assessing size limits for blacklip abalone (*Haliotis rubra*) in Tasmania. In S.A. Shepherd, M. Tegner and S.A. Guzmán del Próo (eds.): *Abalone of the World: biology, fisheries and culture*. pp. 318-338. Blackwell: London.

Population Biology of Blacklip Abalone in Bass Strait

- Nash, W.J., J.C. Sanderson, S.R. Talbot, A. Cawthorn and D. Wikeley, in prep. *a.* Growth and ageing of blacklip abalone (*Haliotis rubra*) in southern Tasmania.
- Nash, W.J., J.C. Sanderson, S. Talbot and A. Cawthorn, in prep. *b.* Stock assessment of blacklip abalone (*Haliotis rubra*) by the change-in-ratio method.
- Pauly, D. 1991. Length-converted catch curves and the seasonal growth of fishes. *Fishbyte* 8(3): 33-38.
- Poore, G. 1972. Ecology of New Zealand abalones, *Haliotis* species (Mollusca; Gastropoda): 3. Growth. *New Zealand Journal of Marine and Freshwater Research* 6: 534-559.
- Prager, M.H., S.B. Saila and C.W. Recksiek 1987. FISHPARM: A microcomputer program for parameter estimation of nonlinear models in fishery science. *Old Dominion University Research Foundation Technical Report* 87-10 : 37 pp.
- Prince, J.D. 1987. The world's abalone fisheries...Lessons for Tasmania. *Report to the Annual General Meeting of the Tasmanian Abalone Divers Association, October 10, 1987.* 23 pp.
- Prince, J.D. 1989. The fisheries biology of the Tasmanian stocks of *Haliotis rubra*. *Ph.D. dissertation, University of Tasmania.* 174 pp.
- Prince, J.D., T.L. Sellers, W.B. Ford and S.R. Talbot 1988a. A method for ageing the abalone *Haliotis rubra* (Mollusca: Gastropoda). *Australian Journal of Marine and Freshwater Research* 39: 167-177.
- Prince, J.D., T.L. Sellers, W.B. Ford and S.R. Talbot 1988b. Recruitment, growth, mortality and population structure in a southern Australian population of *Haliotis rubra* (Mollusca: Gastropoda). *Marine Biology* 100: 75-82.
- Ricker, W.E., 1975. Computation and interpretation of biological statistics of fish populations. *Bulletin of the Fisheries Research Board of Canada* 191: 382 pp.
- Robson, D.S. and D.G. Chapman 1961. Catch curves and mortality rates. *Transactions of the American Fisheries Society* 90: 181-189.
- Sakai, S. 1960. On the formation of the annual ring on the shell of the abalone, *Haliotis discus* var. *hannai*. *Tohoku Journal of Agricultural Research* 11: 239-244.
- Sloan, N.A. and P.A. Breen 1988. Northern abalone, *Haliotis kamtschatkana*, in British Columbia: fisheries and synopsis of life history information. *Canadian Special Publication in Fisheries and Aquatic Sciences* 103: 46 pp.
- Taylor, B.E. and W. Gabriel 1992. To grow or not to grow: optimal resource allocation for *Daphnia*. *The American Naturalist* 139: 248-266.
- Tegner, M.J., P.A. Breen and C.E. Lennert 1989. Population biology of red abalones, *Haliotis rufescens*, in southern California and management of the red and pink, *H. corrugata*, abalone fisheries. *Fishery Bulletin* 87: 313-339.

APPENDIX I. Tables of yield-per-recruit and egg-per-recruit values.

Table A.1. Yield-per-recruit (YPR) values (expressed as a percentage of the maximum weight of a cohort) at several levels of fishing mortality (F) and two sizes at first capture (110 and 118 mm), with $M=Z$ (i.e., assuming $F=0$). YPR values in plain characters are based on a shell layer deposition rate of one per year; values in **bold** characters are based on a shell layer deposition rate of two per year.

Site	Size limit (mm)	<i>F</i>									
		0.2	0.4	0.6	0.8	1.0	1.2	1.4	1.6	1.8	2.0
Hogan Is.	110	48.6 32.9	62.7 48.1	69.0 56.7	72.6 62.1	74.8 65.7	76.3 68.3	77.3 70.3	78.2 71.8	78.8 73.0	79.3 74.0
	118	34.3 22.9	45.1 34.0	50.1 40.4	53.1 44.6	54.9 47.5	56.3 49.6	57.2 51.2	58.0 52.5	58.6 53.5	59.0 54.4
Kent Is.	110	19.7 12.8	26.7 19.6	30.1 23.6	32.2 26.4	33.6 28.3	34.5 29.8	35.2 30.9	35.8 31.8	36.2 32.5	36.6 33.2
	118	7.0 4.6	9.8 7.1	11.2 8.6	12.0 9.7	12.6 10.5	12.9 11.0	13.2 11.5	13.5 11.9	13.7 12.1	13.8 12.4
Babel I.	110	57.2 39.7	71.9 56.7	78.1 65.7	81.3 71.2	83.3 74.8	84.6 77.3	85.6 79.1	86.3 80.5	86.8 81.6	87.3 82.5
	118	45.1 30.9	57.8 44.8	63.4 52.4	66.5 57.2	68.5 60.5	69.8 62.8	70.8 64.5	71.5 65.9	72.1 66.9	72.6 67.8
Cape Barren I.	110	55.3 39.0	68.9 55.0	74.6 63.4	77.6 68.3	79.4 71.6	80.7 73.9	81.6 75.6	82.2 76.9	82.7 77.9	83.1 78.7
	118	40.6 28.4	51.8 40.6	56.7 47.3	59.4 51.4	61.1 54.2	62.2 56.2	63.1 57.7	63.7 58.8	64.3 59.8	64.7 60.5
Waterhouse I.	110	13.0 8.3	17.9 12.9	20.4 15.7	21.9 17.7	22.9 19.1	23.6 20.1	24.2 21.0	24.6 21.6	25.0 22.2	25.2 22.6
	118	1.7 1.2	2.6 1.9	3.1 2.4	3.4 2.7	3.5 2.9	3.7 3.1	3.8 3.2	3.9 3.3	3.9 3.4	4.0 3.5

Table A.2. Yield-per-recruit (YPR) values (expressed as a percentage of the maximum weight of a cohort) at several levels of fishing mortality (F) and two sizes at first capture (110 and 118 mm), with (A) $M = 0.75 \times Z$ (i.e., assuming $F=M+3$) and (B) $M=0.5 \times Z$ (i.e., assuming $F=M$). YPR values in plain characters are based on a shell layer deposition rate of one per year; values in **bold** characters are based on a shell layer deposition rate of two per year.

(A)

Site	Size limit (mm)	F									
		0.2	0.4	0.6	0.8	1.0	1.2	1.4	1.6	1.8	2.0
Hogan Is.	110	64.6 46.5	79.0 64.3	84.6 73.2	87.5 78.4	89.2 81.7	90.3 84.0	91.1 85.6	91.7 86.8	92.1 87.8	92.4 88.5
	118	51.0 36.2	63.8 50.9	69.2 58.7	72.1 63.4	73.9 66.5	75.1 68.7	76.0 70.3	76.7 71.5	77.2 72.5	77.6 73.3
Kent Is.	110	35.8 24.8	46.2 35.8	50.7 41.9	53.3 45.8	55.0 48.4	56.1 50.3	56.9 51.7	57.6 52.8	58.1 53.7	58.5 54.5
	118	16.6 11.8	22.5 17.3	25.1 20.5	26.6 22.5	27.5 23.9	28.2 24.9	28.7 25.7	29.1 26.4	29.4 26.9	29.6 27.3
Babel I.	110	72.8 54.0	86.4 72.5	91.2 81.1	93.5 85.8	94.8 88.7	95.6 90.6	96.1 91.9	96.5 92.8	96.8 93.5	97.0 94.1
	118	62.6 45.7	76.1 62.5	81.3 70.8	84.0 75.6	85.6 78.6	86.7 80.7	87.4 82.2	88.0 83.4	88.4 84.3	88.8 85.0
Cape Barren I.	110	71.4 53.9	84.5 71.5	89.1 79.6	91.4 84.0	92.7 86.8	93.5 88.6	94.1 89.8	94.5 90.8	94.8 91.5	95.0 92.1
	118	58.2 43.5	70.9 58.8	75.7 66.2	78.2 70.6	79.7 73.3	80.8 75.3	81.5 76.7	82.0 77.7	82.4 78.6	82.8 79.2
Waterhouse I.	110	26.3 17.9	34.5 26.3	38.3 31.1	40.5 34.2	41.9 36.4	42.9 38.0	43.6 39.2	44.2 40.1	44.6 40.9	45.0 41.5
	118	5.4 4.4	8.1 6.6	9.5 7.9	10.3 8.7	10.8 9.3	11.1 9.7	11.4 10.1	11.6 10.4	11.7 10.6	11.8 10.8

Table A.2 – continued.

(B)

Site	Size limit (mm)	<i>F</i>									
		0.2	0.4	0.6	0.8	1.0	1.2	1.4	1.6	1.8	2.0
Hogan Is.	110	81.0 63.8	92.6 81.3	96.0 88.5	97.4 92.1	98.1 94.2	98.6 95.5	98.8 96.3	99.0 96.9	99.1 97.3	99.2 97.6
	118	71.4 55.3	84.0 72.0	88.3 79.5	90.4 83.6	91.7 86.2	92.5 87.9	93.0 89.1	93.4 90.0	93.8 90.7	94.0 91.2
Kent Is.	110	59.8 45.5	72.5 60.7	77.1 68.0	79.5 72.1	80.9 74.8	81.9 76.7	82.6 78.0	83.1 79.0	83.5 79.8	83.8 80.4
	118	36.1 28.7	46.9 39.0	51.0 44.2	53.1 47.4	54.4 49.4	55.2 50.9	55.8 52.0	56.3 52.8	56.6 53.5	56.9 54.0
Babel I.	110	86.3 70.4	95.6 86.7	97.6 92.5	98.2 95.1	98.4 96.4	98.4 97.1	98.4 97.5	98.3 97.7	98.3 97.8	98.2 97.9
	118	80.7 64.7	92.1 81.5	95.4 88.3	96.8 91.7	97.6 93.7	98.0 94.9	98.3 95.8	98.5 96.4	98.7 96.8	98.8 97.1
Cape Barren I.	110	85.8 71.1	95.5 86.8	97.8 92.6	98.6 95.2	98.9 96.5	99.1 97.3	99.2 97.8	99.2 98.1	99.2 98.3	99.2 98.5
	118	77.3 63.5	89.4 79.3	92.9 85.8	94.4 89.2	95.3 91.2	95.8 92.5	96.2 93.3	96.5 94.0	96.7 94.5	96.8 94.9
Waterhouse I.	110	49.2 36.7	60.8 50.0	65.4 56.6	67.8 60.6	69.3 63.1	70.3 65.0	71.0 66.3	71.6 67.4	72.0 68.2	72.4 68.8
	118	15.6 14.9	23.0 20.7	26.7 23.7	28.6 25.6	29.7 26.9	30.4 27.8	30.9 28.5	31.2 29.0	31.5 29.5	31.7 29.8

Table A.3. Egg-per-recruit (EPR) values (expressed as a percentage of the egg production in the absence of fishing) at several levels of fishing mortality (F) and two sizes at first capture (110 and 118 mm), with $M=Z$ (i.e., assuming $F=0$). EPR values in plain characters are based on a shell layer deposition rate of one per year; values in **bold** characters are based on a shell layer deposition rate of two per year.

Site	Size limit (mm)	F									
		0.2	0.4	0.6	0.8	1.0	1.2	1.4	1.6	1.8	2.0
Hogan Is.	110	70.6 79.3	60.7 69.2	55.8 63.3	53.0 59.4	51.2 56.7	49.9 54.7	49.0 53.1	48.3 51.9	47.7 50.9	47.2 50.1
	118	81.1 86.3	74.3 79.5	70.9 75.4	68.9 72.7	67.6 70.8	66.6 69.4	65.9 68.3	65.4 67.4	65.0 66.7	64.6 66.1
Kent Is.	110	89.5 92.5	85.4 88.5	83.2 86.0	81.9 84.3	81.0 83.1	80.4 82.2	79.9 81.4	79.6 80.9	79.3 80.4	79.0 80.0
	118	97.1 97.4	95.7 96.0	95.0 95.2	94.5 94.6	94.2 94.1	94.0 93.8	93.8 93.5	93.6 93.3	93.5 93.1	93.4 93.0
Babel I.	110	70.3 78.5	60.7 68.5	56.2 62.8	53.7 59.1	52.0 56.6	50.8 54.8	50.0 53.4	49.3 52.3	48.8 51.4	48.4 50.6
	118	78.7 84.2	71.4 76.7	67.9 72.4	65.9 69.6	64.6 67.6	63.6 66.2	63.0 65.1	62.4 64.2	62.0 63.5	61.7 62.9
Cape Barren I.	110	72.5 78.9	63.6 69.5	59.5 64.2	57.1 60.9	55.6 58.6	54.6 57.0	53.8 55.7	53.2 54.7	52.7 53.9	52.4 53.3
	118	82.5 85.6	76.2 79.1	73.3 75.4	71.6 73.0	70.4 71.4	69.7 70.2	69.1 69.2	68.6 68.5	68.3 67.9	68.0 67.4
Waterhouse I.	110	94.0 95.8	91.5 93.4	90.2 91.9	89.4 90.9	88.8 90.1	88.4 89.6	88.1 89.1	87.9 88.8	87.7 88.5	87.6 88.2
	118	99.6 99.4	99.2 99.1	99.1 98.8	99.0 98.7	98.9 98.6	98.9 98.5	98.9 98.4	98.8 98.4	98.8 98.3	98.8 98.3

Table A.4. Egg-per-recruit (EPR) values (expressed as a percentage of the egg production in the absence of fishing) at several levels of fishing mortality (F) and two sizes at first capture (110 and 118 mm), with (A) $M = 0.75 \times Z$ (i.e., assuming $F=M+3$) and (B) $M=0.5 \times Z$ (i.e., assuming $F=M$). EPR values in plain characters are based on a shell layer deposition rate of one per year; values in **bold** characters are based on a shell layer deposition rate of two per year.

(A)

Site	Size limit (mm)	F									
		0.2	0.4	0.6	0.8	1.0	1.2	1.4	1.6	1.8	2.0
Hogan Is.	110	62.0 70.7	50.7 58.4	45.7 51.8	42.8 47.7	41.0 44.9	39.8 43.0	38.9 41.5	38.2 40.3	37.7 39.4	37.2 38.6
	118	73.4 78.4	64.7 69.2	60.7 64.1	58.5 60.9	57.0 58.7	56.0 57.2	55.3 56.0	54.7 55.0	54.2 54.3	53.9 53.7
Kent Is.	110	82.7 85.9	76.5 79.4	73.5 75.7	71.8 73.3	70.7 71.7	69.9 70.5	69.3 69.5	68.8 68.8	68.5 68.2	68.2 67.7
	118	94.2 93.7	91.6 90.7	90.2 88.9	89.3 87.8	88.8 87.0	88.4 86.4	88.1 86.0	87.9 85.6	87.7 85.3	87.5 85.1
Babel I.	110	61.2 69.2	50.3 57.0	45.6 50.6	43.0 46.8	41.4 44.2	40.3 42.4	39.5 41.0	38.8 40.0	38.4 39.1	38.0 38.5
	118	70.3 75.5	61.3 65.5	57.3 60.3	55.0 57.0	53.6 54.8	52.6 53.3	51.9 52.1	51.4 51.2	50.9 50.4	50.6 49.9
Cape Barren I.	110	64.4 69.6	54.2 58.1	49.7 52.3	47.3 48.8	45.8 46.4	44.7 44.8	44.0 43.5	43.4 42.6	42.9 41.8	42.6 41.2
	118	75.6 77.2	67.7 68.3	64.1 63.7	62.1 60.9	60.8 59.0	60.0 57.7	59.3 56.7	58.8 55.9	58.5 55.3	58.1 54.8
Waterhouse I.	110	88.8 90.9	84.6 86.5	82.4 83.9	81.2 82.2	80.4 81.1	79.8 80.2	79.4 79.5	79.0 79.0	78.8 78.5	78.6 78.2
	118	99.0 97.9	98.3 96.8	97.9 96.2	97.7 95.8	97.5 95.5	97.3 95.3	97.2 95.1	97.1 95.0	97.0 94.9	97.0 94.8

Population Biology of Blacklip Abalone in Bass Strait

Table A.4 – continued.

(B)

Site	Size limit (mm)	<i>F</i>									
		0.2	0.4	0.6	0.8	1.0	1.2	1.4	1.6	1.8	2.0
Hogan Is.	110	52.1 58.0	39.9 44.2	35.0 37.6	32.3 33.7	30.7 31.3	29.6 29.5	28.8 28.3	28.2 27.3	27.7 26.5	27.4 25.9
	118	63.8 65.8	53.5 54.2	49.1 48.5	46.7 45.2	45.2 43.0	44.2 41.4	43.4 40.3	42.9 39.4	42.4 38.7	42.1 38.2
Kent Is.	110	73.2 73.7	64.7 64.1	60.9 59.2	58.8 56.3	57.4 54.4	56.5 53.0	55.9 51.9	55.3 51.1	54.9 50.5	54.6 50.0
	118	89.3 84.6	84.7 78.7	82.4 75.7	81.0 73.8	80.2 72.6	79.5 71.7	79.1 71.0	78.8 70.5	78.5 70.1	78.3 69.8
Babel I.	110	51.0 55.8	39.3 42.2	34.6 35.9	32.2 32.3	30.7 30.0	29.7 28.5	29.0 27.3	28.4 26.5	28.0 25.8	27.7 25.3
	118	60.3 62.0	49.8 50.0	45.5 44.3	43.2 41.0	41.7 38.9	40.8 37.4	40.1 36.3	39.5 35.5	39.1 34.9	38.8 34.3
Cape Barren I.	110	55.4 56.4	44.1 43.6	39.6 37.7	37.2 34.4	35.7 32.3	34.7 30.9	34.0 29.8	33.5 29.0	33.1 28.4	32.7 27.9
	118	67.4 64.1	57.7 53.1	53.7 48.0	51.5 45.1	50.1 43.2	49.2 41.9	48.5 40.9	48.0 40.2	47.6 39.6	47.3 39.1
Waterhouse I.	110	80.4 80.5	73.8 72.9	70.7 69.0	69.0 66.6	67.9 65.0	67.2 63.8	66.6 62.9	66.2 62.3	65.8 61.7	65.6 61.3
	118	97.6 92.7	96.2 89.7	95.2 88.2	94.6 87.2	94.2 86.5	93.9 86.1	93.6 85.7	93.5 85.4	93.3 85.2	93.2 85.0